PERFORMANCE CURVES OF A DOUBLE-CAGE INDUCTION MOTOR

A THESIS

Presented to

the Faculty of the Division of Graduate Studies

Georgia School of Technology

In Partial Fulfillment

of the Requirements for the Degree

Master of Science in Electrical Engineering

by

James Hubert Noland, Jr.

June 1948

PERFORMANCE CURVES OF A DOUBLE-CAGE INDUCTION MOTOR

Approved:

Date Approved by Chairman May 31, 1948

ACKNOWLEDGEMENT

This thesis would not be complete without an expression of my appreciation to Dean D. P. Savant, both for his initial suggestion of the problem and for his additional advice throughout its pursuit.

TABLE OF CONTENTS

TABLE OF CONTENTS (Continued)

LIST OF TABLES

LIST OF FIGURES

LIST OF SYMBOLS USED

All constants used, with the exception of V_t, the terminal voltage, and P_{in}, the total power input, are on a per phase basis. All quantities pertaining to the rotor are referred to the stator.

a .... constant expressing per-unit increase in effective stator resistance per ten cycle increase of applied frequency.

b_m ... magnetizing susceptance.

c .... ratio of effective resistance of outer cage to d-c resistance of rotor.

E .... voltage induced in rotor, referred to stator.

f .... frequency.

g_m ... magnetizing conductance.

I .... line current.

I_n ... ideal no-load current (mechanical losses equal zero).

N .... speed, rpm.

P_2 ... power transferred to the rotor.

P_2' ... power delivered to rotor copper.

P_{cu_1} . power lost in stator copper.

P_{cu_2} . power lost in rotor copper.

P_f ... friction and windage loss.

P_{fe_1} . stator iron loss.

P_h ... hystersis loss in rotor.

P_{in} .. total power input.

P_i ... power input per phase.

P_i' ... power input per phase less stator copper loss.

P_o ... power output.

P_p ... flux pulsation loss.

R_1 ... effective stator resistance.

R_{1_1} .. effective stator resistance at test frequency f_1.

R_{1_2} .. effective stator resistance at test frequency f_2.

R_{1dc} .. direct-current resistance of stator.

R_2 ... effective rotor resistance.

R_{2_1} .. effective rotor resistance at test frequency f_1.

R_{2_2} .. effective rotor resistance at test frequency f_2.

R_{2dc} .. direct-current resistance of rotor.

R_b ... fictitious resistance used in equivalent circuit of Figure 12.

R_{eq} .. equivalent resistance of motor.

R_i ... effective resistance of inner cage.

R_m ... core loss component of magnetizing impedance.

R'_m ... core loss component of magnetizing impedance when connected across the motor terminals.

R_o ... effective resistance of outer cage.

R'_o ... fictitious resistance of outer cage as used in equivalent circuit of Figure 12.

s .... slip.

V .... applied voltage per phase.

V_t ... terminal voltage.

v .... ratio of inner cage reactance to its effective resistance.

X_1 ... stator reactance.

X_2 ... equivalent rotor reactance.

X_b ... common reactance of both cages, due to mutual flux.

X_{eq} .. equivalent reactance of motor.

X_i ... reactance of inner cage, due to flux linking it alone.

X'_i ... fictitious reactance of inner cage, used in equivalent circuit of Figure 12.

X_{it} .. total reactance of inner cage.

X_m ... magnetizing reactance, when connected between stator and rotor.

X'_m ... magnetizing reactance, when connected across the motor terminals.

X_o ... reactance of outer cage, due to flux linking it alone.

X_{o_t} .. total reactance of outer cage.

Y .... total admittance of motor.

Y_i ... admittance of inner cage.

Y_m ... magnetizing admittance.

Y_o ... admittance of outer cage.

Y_{oi} .. admittance of outer and inner cages in parallel.

Z_1 ... stator impedance.

Z_2 ... equivalent impedance of rotor.

Z' ... auxiliary impedance of motor, defined in equation 34, page 32.

Z_{eq} .. equivalent impedance of entire machine.

Z_i ... impedance of inner cage.

Z_m ... magnetizing impedance, when connected between rotor and stator.

Z'_m ... magnetizing impedance, when connected across motor terminals.

Z_o ... impedance of the outer cage.

α.... angle of which tangent is $R_1/X_1 + X_m$.

τ_1 ... primary leakage coefficient, X_1/X_m.

PERFORMANCE CURVES OF A DOUBLE-CAGE INDUCTION MOTOR

CHAPTER I

THE PROBLEM AND REVIEW OF PREVIOUS WORK

Statement of the problem. It is very desirable to be able to predict the operating characteristics of electrical machinery from tests which do not require a great amount of power. With most apparatus this causes little difficulty, but the double squirrel-cage induction motor, with its many variable elements, poses a somewhat greater problem.

It was the purpose of this study, therefore, (1) to set forth several methods of obtaining a current diagram for the double-cage motor analogous to the circle diagram for the normal three-phase motor; (2) to obtain from the current diagram the desired operating characteristic curves; and (3) to compare the results as to the relative merits of the various methods used.

Review of previous work. There is very little work in American publications on an actual mathematical analysis of the double cage machine. Most American authors describe the rotor bar configuration, explain how the high resistance cage is effective on starting and the low resistance cage on running, draw a torque-slip characteristic, and let it go at that. The first really big installation--that on the United States Battleship New Mexico--is rather completely described in the General Electric Review,[1] but this particular problem of predicting

[1] E. F. W. Alexanderson, "General Characteristics of Ship Propulsion Apparatus," General Electric Review, 22:224-32, April, 1919.

the characteristics is not covered. Behrend, who claimed to have originated the circle diagram for the three-phase induction motor, also shows a current diagram for the double-cage machine, but plots it point by point from the impedance equation rather than by a geometrical construction.[2]

The AIEE test code treats the double-cage machine very much as the ordinary three-phase induction motor, but with a special method of finding the rotor and stator reactances.[3]

Equivalent circuits were published by Steinmetz[4] in 1917, Behrend[5] in 1921, and T. F. Wall[6] in 1923, all differing in some degree. These will be discussed at greater length in Chapter II, since the admittance diagram of some form of equivalent circuit forms the basis for the desired current diagram.

Several forms of current diagrams were published in German periodicals between 1928 and 1932. One of these is given by Punga, who used it primarily as an aid in the design of the machine to meet desired starting and running conditions.[7] A discussion and diagram was given

---

[2] B. A. Behrend, The Induction Motor (New York: McGraw-Hill Book Company, Inc., 1921), p.120.

[3] AIEE Test Code for Polyphase Induction Machines (AIEE Standards, No. 500, New York: American Institute of Electrical Engineers, 1937) pp. 1-25.

[4] Charles P. Steinmetz, Theory and Calculation of Electrical Apparatus (New York: McGraw-Hill Book Company, Inc., 1917), pp. 29-34.

[5] Behrend, op. cit., p. 117.

[6] T. F. Wall, "Squirrel Cage Induction Motors with High Starting Torque and Low Starting Current," Engineering, (London), 116:164-66, August 10, 1923.

[7] Franklin Punga, "Die günstigste Dimensionierung des Boucherot-Motors," Archiv für Elektrotechnik, 21:1, January 1928. Franklin Punga and Otto Raydt, Modern Polyphase Induction Motors (London: Sir Isaac Pitman & Sons, Ltd., 1933), pp. 61-84.

by Baffrey at about the same time.[8] These were cited by Krondl, who then stated his intention to develop a simpler--though no less accurate--current diagram.[9] His method will be utilized later in developing the most accurate diagram given herein.

Two even simpler diagrams were given by Say and Pink in an English text. These are based on approximate forms of the equivalent circuits.[10]

An entirely different approach is that of Örley and Jekelfalussy in the Hungarian Elektrotechnika in 1946; it provides a set of charts which may be used on any double-cage machine, and which are primarily for determining machine constants to fulfill required operating conditions, but which could be used in the reverse manner.[11]

All of these methods depend on knowing the values of the constants involved in the equivalent circuit. The only method found for obtaining these from test data is given by Hanskarl Voigt and makes use of blocked-rotor tests at a number of frequencies.[12]

Method of approach. First, complete tests to determine the basic constants of the machine as prescribed by Voigt were performed. These are described in Chapter III. Then current diagrams were drawn

---

[8] R. Baffrey, "Der Koppelkäfigankermotor," Elektrotechnik und Maschinenbau, 46:749-54, July 8, 1928.

[9] Milan Krondl, "Das Arbeitsdiagramm des Boucherot-Motors," Elektrotechnik und Maschinenbau, 49:161-67, March 1, 1931.

[10] M. G. Say and E. N. Pink, The Performance and Design of Alternating Current Machines (London: Sir Isaac Pitman & Sons, Ltd., 1936), p. 274.

[11] D. Örley and G. Jekelfalussy, "Practical Design of Double Squirrel Cage Motors," Engineers' Digest, 4:253-56, June 1947. Translation from Elektrotechnika, 38:108-13, December 15, 1946.

[12] Hanskarl Voigt, "Die Trennung der Widerstände eines Doppelkäfig-Ankers," Elektrotechnik und Maschinenbau, 50:133-35, February 28, 1932.

utilizing several different methods, and the performance curves predicted, as shown in Chapters IV and V. These predicted values were checked against an actual brake test on the machine, and at large slips check values were obtained by measuring instantaneous values of current and slip during starting and coming up to speed.

No two references consulted used the same system of symbols. The system given in the preface is not identical with any one, but is an attempt to give one which agrees so far as possible with accepted American notation, with the special symbols required clear as to their meaning.

CHAPTER II

THE EQUIVALENT CIRCUIT

Since all methods of predicting characteristics are based on some form of equivalent circuit, the various types will be discussed first.

Behrend's equivalent circuit. The circuit set forth by Behrend is based on the leakage flux method of Blondel, rather than the more generally used leakage reactances.[1] Since this method is no longer used in this country to any appreciable degree, the circuit is not reproduced here.

Steinmetz's equivalent circuit. Probably the originator of the equivalent circuit method of representing the double cage machine was Steinmetz, who first suggested this method for the ordinary induction motor.[2] In his book of 1917, the circuit is not actually published, but the equations used in the development of current and power relationships show that he had in mind a circuit of the form of Figure 1.[3] This circuit neglects the reactance due to flux linking the outer cage alone, which with the rotor bar configuration of Figure 2 is very small,[4] since it can be seen from this Figure that the flux does not exist in

---

[1] B. A. Behrend, The Induction Motor (New York: McGraw-Hill Book Company, Inc., 1921), pp. 115-17.

[2] Albert F. Puchstein and Tom C. Lloyd, Alternating Current Machines (New York: John Wiley & Sons, Inc., 1942), p. 145.

[3] Charles P. Steinmetz, Theory and Calculation of Electrical Apparatus (New York: McGraw-Hill Book Company, Inc., 1917), p. 29.

[4] Franklin Punga and Otto Raydt, Modern Polyphase Induction Motors (London: Sir Isaac Pitman & Sons, Ltd., 1933), p. 62.

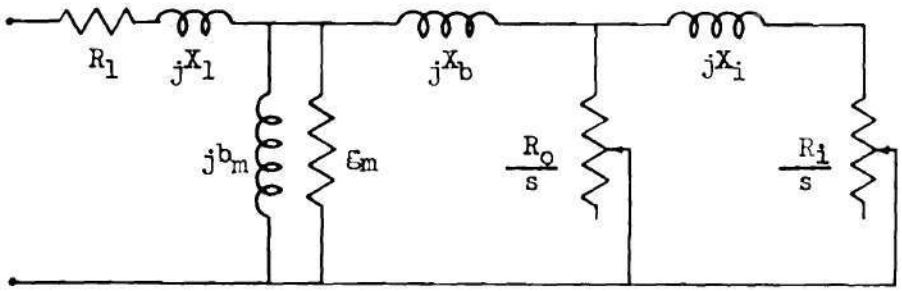

Where $R_1 + jX_1$ - stator impedance.

$g_m + jb_m$ = magnetizing admittance.

R_o - effective resistance of outer cage.

R_i = effective resistance of inner cage.

X_i = Reactance of inner cage due to flux linking it alone.

X_b = common reactance of both cages due to mutual flux.

s = slip.

FIGURE 1

STEINMETZ'S EQUIVALENT CIRCUIT

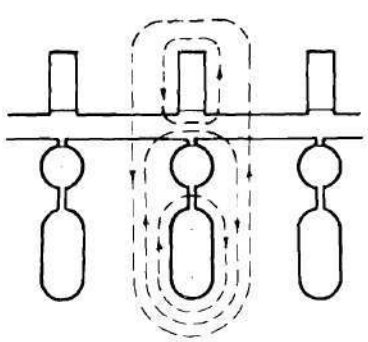

FIGURE 2

FLUX DISTRIBUTION WITH "DUMBBELL" SLOTTING

in the iron but only inside the bar itself. This circuit and modifications of it are those most generally used in the development of the current diagrams.

Wall's equivalent circuit. In the equivalent circuit as set forth by Wall, each cage is treated as a separate motor and the rotor current and torque found by summing up the components for each cage.[5] This method neglects the mutual effect between the two cages, which is rather large for slottings of the form of Figure 2, though less for other forms such as Figure 3. This equivalent circuit is shown in Figure 4. A simple current diagram has been developed from it, with the further simplification of assuming zero stator impedance.[6]

Other modifications can be made to these equivalent circuits, and some will be shown later in the development of the current diagrams.

---

[5] T. F. Wall, "Squirrel Cage Induction Motor with High Starting Torque and Low Starting Current," Engineering (London), 116:165, August 10, 1923.

[6] M. G. Say and E. N. Pink, The Performance and Design of Alternating Current Machines (London: Sir Isaac Pitman & Sons, Ltd., 1936), p. 274.

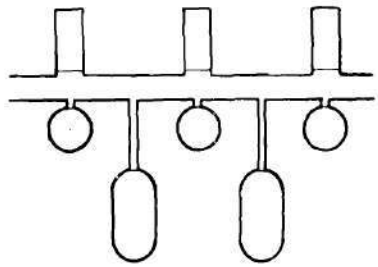

FIGURE 3

"STAGGERED" SLOTTING

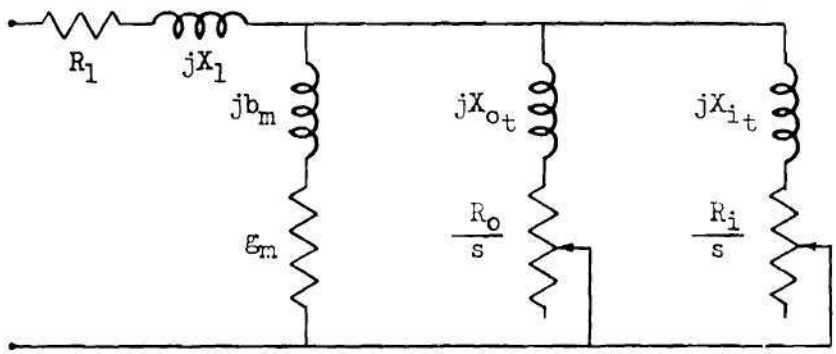

where $R_1 + jX_1$ = stator impedance.

$g_m + jb_m$ = magnetizing admittance.

$R_o + jX_{o_t}$ = total impedance of outer cage.

$R_i + jX_{i_t}$ = total impedance of inner cage.

s = slip.

FIGURE 4

WALL'S EQUIVALENT CIRCUIT

CHAPTER III

DETERMINATION OF THE CONSTANTS OF THE MACHINE

The remainder of this thesis is a report of tests performed on a three-phase, double-cage, 7.5 HP induction motor manufactured by the Louis Allis Company of Milwaukee, Wisconsin. The nameplate data of this machine is given in Table I, page 12.

Since, as previously stated, the current diagram is based on the equivalent circuit, the initial problem is to determine the values of the effective resistances and reactances of the stator and the two cages. Were the physical dimensions of the slots and the winding data known, these could conceivably be calculated. Here, however, it was desired to determine these values by actual tests on the machine, to provide for the case where the design data is unavailable or where it is desired to check actual performance against the original design.

Separation of resistances of the two cages. The method developed by Voigt for separating the resistances of the two cages,[1] derivation of which is given in Appendix I, pp. 56-59, is based on the Steinmetz equivalent circuit shown in Figure 1. Blocked rotor tests are required to be made at a number of frequencies, and the following relationships are used to separate the resistances:

$$R_o = cR_{2dc} \tag{1}$$

$$R_i = \frac{R_o}{c - 1} \tag{2}$$

$$X_i = vR_i \tag{3}$$

---

[1] Hanskarl Voigt, "Die Trennung der Widerstande eines Doppelkafig-Ankers," Elektrotechnik und Maschinenbau, 50:133-35, February 28, 1932.

where

$$c = \frac{(f_1/f_2)^2 R_{2_1}(R_{2_2} - R_{2dc}) - R_{2_2}(R_{2_1} - R_{2dc})}{R_{2dc}\left[(f_1/f_2)^2(R_{2_2} - R_{2dc}) - (R_{2_1} - R_{2dc})\right]} \tag{4}$$

$$v = c\sqrt{\frac{R_{2_1} - R_{2dc}}{cR_{2dc} - R_{2_1}}} \tag{5}$$

R_{2dc} = d-c resistance of rotor.

R_{2_1} = effective resistance of rotor at test frequency f_1.

R_{2_2} = effective resistance of rotor at test frequency f_2.

R_i = effective resistance of inner cage.

R_o = effective resistance of outer cage.

X_i = reactance of inner cage.

All rotor values are referred to the stator.

Determination of rotor direct-current resistance. The above relationships require, besides the data obtained from the multiple frequency blocked rotor test, the knowledge of the d-c resistance of the rotor referred to the stator. This was also found by a method developed by Voigt, and utilizes tests performed at very light loads.[2]

The power input, slip, and line current is measured at no load and under very small loads, and a curve plotted of input power less stator copper loss versus slip. The rotor resistance is then calculated from the expression derived in Appendix II, page 56,

$$R_{2dc} = E^2\frac{\Delta s}{\Delta P_2'} \tag{6}$$

where E = rotor voltage referred to stator.

$\frac{\Delta P_2'}{\Delta s}$ = slope of the above curve as slip approaches zero.

---

[2] Hanskarl Voigt, "Vereinfachung des Leerlaufverfahrens zur Bestimmung des Läuferwiderstandes von Asynchronmotoren," Elektrotechnik und Maschinenbau, 49:167-68, March 1, 1931.

In this particular case, the test was performed as prescribed, and the data recorded in Table III. The desired curve is plotted in Figure 6, page 16, and from it was obtained:

$$\frac{\Delta P_2'}{\Delta s} = \frac{293}{0.003} = \frac{1}{0.00001017} \tag{7}$$

From the 60-cycle blocked rotor test, Table II and Figure 5, it was found that

$$X_{eq} = 1.19 \text{ ohm}$$
$$X_1 = 0.4 \times X_{eq} = 0.476 \text{ ohm.}^3 \tag{8}$$

Where V equals phase voltage,[4]

$$E = V - IX_1 \tag{9}$$
$$= \frac{228}{\sqrt{3}} - 10.3 \times 0.476 = 126.5 \text{ volts.}$$
$$R_{2dc} = \frac{\Delta s}{\Delta P_2'} E^2 = 0.00001017 \times 126.5^2 \tag{10}$$
$$= 0.163 \text{ ohm.}$$

This resistance must be converted to the same temperature as prevailed during the blocked rotor test. From d-c resistance measurements, the cold stator resistance per phase was 0.144 ohm; after the blocked test it was 0.156 ohm, while after the no-load test it was 0.150 ohm. Assuming an equal rise of temperature in both rotor and stator and the same temperature coefficient, we have the proportion

$$\frac{R_{2dc}}{0.163} = \frac{0.156}{0.150}; \quad R_{2dc} = 0.170 \text{ ohm.} \tag{11}$$

---

3 AIEE Test Code for Polyphase Induction Machines (AIEE Standards No. 500. New York: American Institute of Electrical Engineers, 1937), p. 21.

4 Ralph R. Lawrence, Principles of Alternating-Current Machinery (New York: McGraw-Hill Book Company, Inc., 1940), p.485.

TABLE I

NAMEPLATE DATA

Induction Motor Serial No. 882544

Phase	3
Cycle	60
Horsepower	7.5
Volts	220/440
Current	21.4/10.7
RPM	1760

Manufactured by

THE LOUIS ALLIS CO.

Milwaukee, Wis.

TABLE II

60-CYCLE BLOCKED ROTOR TEST

Line current	Terminal voltage	Power input	Equivalent resistance	Equivalent impedance	Equivalent reactance
I	V_t	P_{in}	$R_{eq} = \frac{P_{in}}{3I^2}$	$Z_{eq} = \frac{V_t}{\sqrt{3}I}$	$X_{eq} = \sqrt{Z^2 - R^2}$
amperes	volts	watts	ohms	ohms	ohms
6.9	15.8	72	0.504	1.322	1.223
9.8	21.8	148	0.514	1.285	1.177
12.9	29.4	272	0.544	1.314	1.195
15.7	35.3	400	0.540	1.300	1.182
18.3	41.2	540	0.537	1.292	1.178
19.8	44.7	650	0.552	1.302	1.181
21.7	49.1	780	0.551	1.307	1.182
23.8	53.9	940	0.553	1.307	1.184
25.8	59.1	1130	0.565	1.320	1.192

Before test: $R_{1dc} = 0.144$ ohms per phase.
After test: $R_{1dc} = 0.156$ ohms per phase.

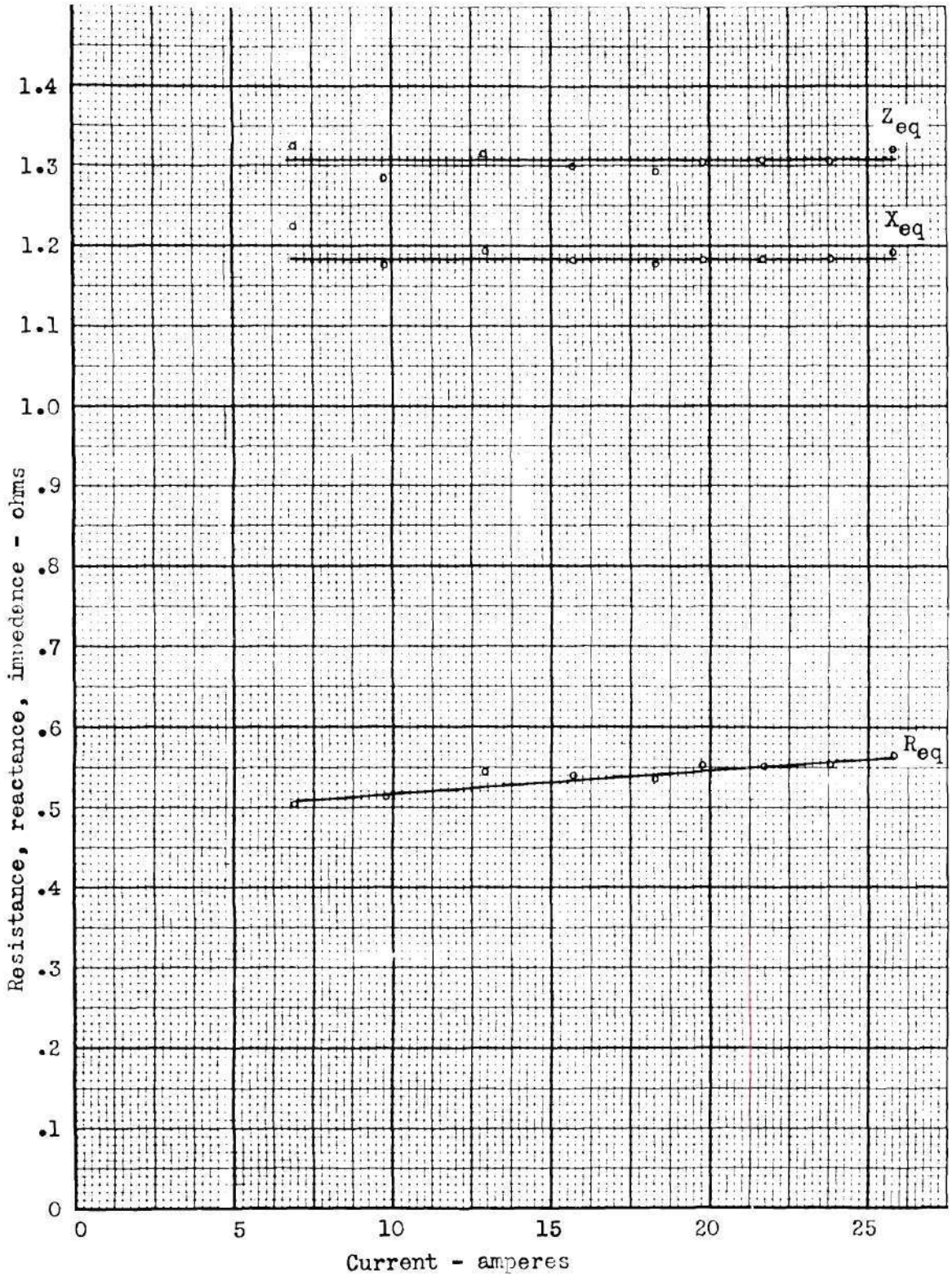

FIGURE 5

60-CYCLE BLOCKED ROTOR TEST

TABLE III

LIGHT-LOAD TEST TO DETERMINE DIRECT-CURRENT RESISTANCE OF ROTOR

Speed	Average line current	Terminal voltage	Power input	P_{in} per phase	Stator copper loss	$P_i - I^2R_1$	Slip
N	I	V_t	P_{in}	P_i	I^2R_1	P_i'	s
RPM	amperes	volts	watts	watts	watts	watts	
1799.5	10.1	228	316	105	19	86	.00026
1797.3	10.2	228	611	204	19	185	.00150
1795.0	10.5	228	1050	350	21	329	.00278
1794.7	10.5	228	1108	369	21	348	.00294
1794.2	10.7	228	1190	397	21	376	.00322
1793.5	10.8	228	1320	440	22	418	.00361
1793.3	10.9	228	1390	464	22	442	.00372
1792.7	11.1	228	1520	507	23	484	.00405
1791.8	11.3	228	1920	640	24	616	.00455
1797.0	10.4	228	684	228	20	208	.00167
1799.5	10.3	228	300	100	20	80	.00028

Before test: $R_{1dc} = 0.144$ ohms per phase.
After test: $R_{1dc} = 0.150$ ohms per phase.

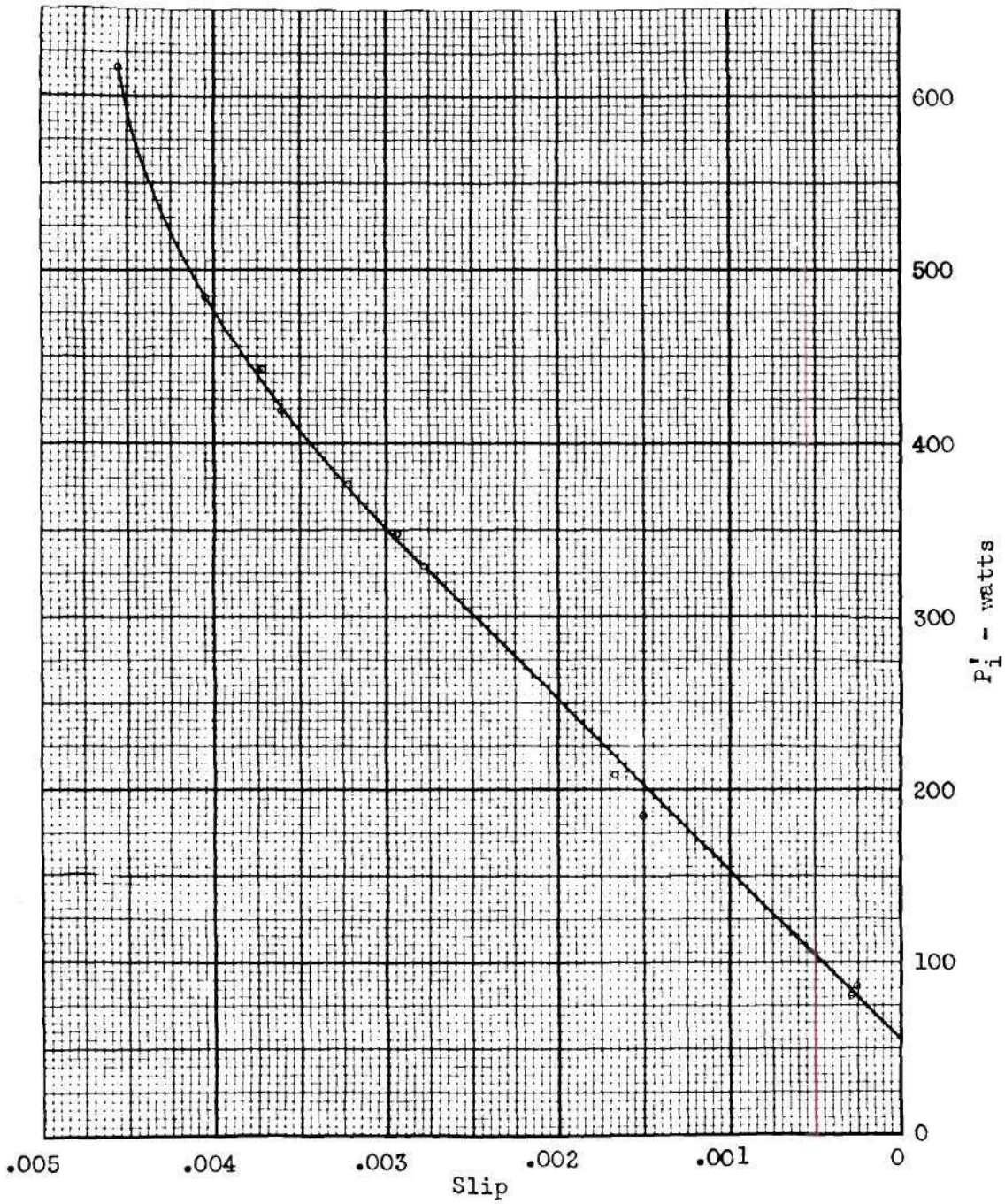

FIGURE 6

TEST TO DETERMINE DIRECT-CURRENT RESISTANCE OF ROTOR

Separation of effective rotor and stator resistances. The above method for separation of the cage resistances requires the knowledge of effective rotor resistance; the blocked rotor test gives equivalent resistance of rotor and stator in series. The stator d-c resistance is easily found, but the ratio of effective to d-c resistance is unknown. With the deep rotor slots it is of course impossible to assume as is often done that the ratio is the same in both rotor and stator.

This difficulty was overcome by taking the data from three frequencies of the blocked rotor test, and so adjusting the stator effective resistance that the constant "c" calculated from equation (4) for two pair of these was the same.

From the shape of the general curve of effective resistance vs. frequency,[5] it was assumed that the stator resistance remained constant from zero to ten cycles, and then increased linearly with frequency. This assumption is expressed by the relation

$$R_{1_1} = R_{1dc}\left[1 + (f_1 - 10)a\right] \tag{12}$$

where "a" is a constant.

Then,

$$R_{2_1} = R_{eq_1} - R_{1_1} = R_{eq_1} - R_{1dc}\left[1 + (f_1 - 10)a\right] \tag{13}$$

It was originally intended to substitute this expression of equation (13) into equation (4), set the value of "c" equal to that obtained from another pair of frequencies, and solve for "a". However, this led to a fourth power equation, so instead a trial and error method was used to obtain approximately equal values of "c". This gave, using the data from 60, 50, and 20 cycles, a value for "a" of 0.004, which at

---

[5] Standard Handbook for Electrical Engineers (New York: McGraw-Hill Book Company, Inc., 1941), Sec. 4-29, 48.

60 cycles gives a ratio of 1.2 between effective and d-c resistance.

The values of "c" from the remaining frequencies were then calculated and averaged, giving an average of 3.57. These calculations are tabulated in Table V, page 21.

From the relationships given on page 9,

$$R_o = cR_{2dc} = 3.57 \times 0.170 = 0.607 \text{ ohm} \tag{14}$$

$$R_i = \frac{R_o}{c - 1} = \frac{0.607}{2.57} = 0.236 \text{ ohm} \tag{15}$$

$$v = c\sqrt{\frac{R_{2_1} - R_{2dc}}{cR_{2dc} - R_{2_1}}} = 3.57\sqrt{\frac{0.361 - 0.170}{3.57 \times 0.170 - 0.361}} \tag{16}$$

$$= 3.14$$

$$X_i = vR_i = 3.14 \times 0.236 = 0.741 \text{ ohm} \tag{17}$$

From equation (A24), Appendix I,

$$X_{eq} = X_1 + X_b + R_o v \frac{c - 1}{c^2 + v^2} \tag{18}$$

$$1.19 = 0.476 + X_b + 0.607 \times 3.14 \frac{2.57}{3.57^2 + 3.14^2}$$

$$X_b = 0.497 \text{ ohm.}$$

From Table V, $R_1 = 0.187$ ohm.

Determination of friction and windage loss. Following the AIEE method,[6] a no-load test at different voltages was performed to evaluate the friction and windage loss. The data is recorded in Table VI, page 22, and a plot of power input vs. voltage applied is shown in Figure 8, page 23. Extrapolating this curve back to the ordinate of zero voltage, the intercept gives friction and windage loss, since core and copper

[6] AIEE Test Code for Polyphase Induction Machines (AIEE Standards No. 500. New York: American Institute of Electrical Engineers, 1937), p. 8.

TABLE IV

VARIABLE-FREQUENCY BLOCKED-ROTOR TEST

Freq.	Line current	Terminal voltage	Power input	Equivalent resistance	Equivalent impedance	Equivalent reactance
f	I	V_t	P_{in}	$R_{eq} = \frac{P_{in}}{3I^2}$	$Z_{eq} = \frac{V_t}{\sqrt{3}I}$	$X_{eq} = \sqrt{Z^2 - R^2}$
cps	amperes	volts	watts	ohms	ohms	ohms
60	19.65	44.1	624	0.538	1.294	1.179
55	19.96	42.7	632	0.529	1.233	1.112
50	19.80	37.7	584	0.496	1.098	0.979
45	19.80	35.6	564	0.480	1.037	0.917
40	19.88	33.2	548	0.462	0.965	0.847
35	19.90	30.8	520	0.438	0.893	0.778
30	20.10	28.3	496	0.409	0.812	0.702
25	20.20	25.7	476	0.389	0.734	0.621
20	19.90	22.5	432	0.364	0.652	0.540
15	20.50	19.7	428	0.340	0.554	0.437

Before test: $R_{1dc} = 0.144$ ohms per phase.
After test: $R_{1dc} = 0.157$ ohms per phase.

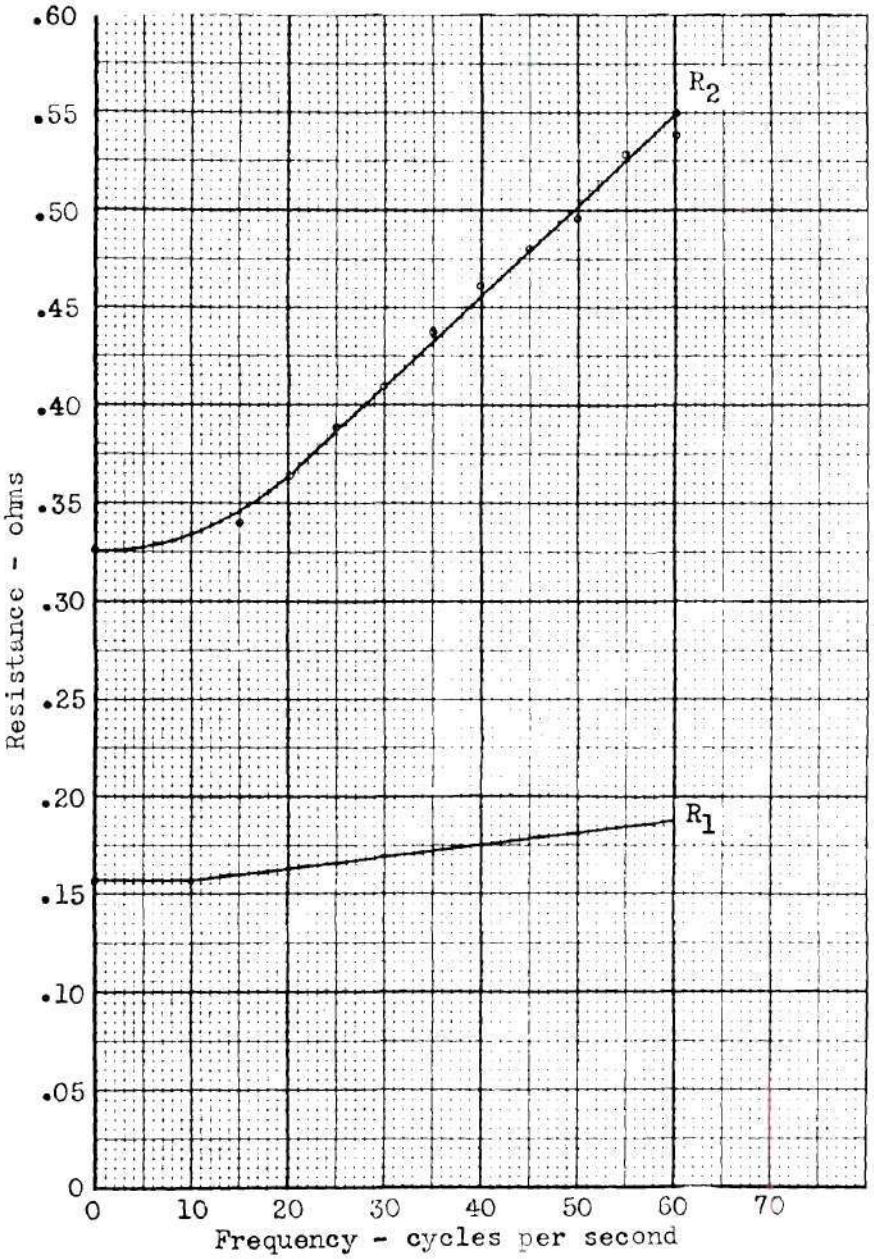

FIGURE 7

STATOR AND ROTOR RESISTANCE VS. FREQUENCY

TABLE V

CALCULATIONS TO DETERMINE c

Freq. f	$\frac{f_1}{f_2}$	Equivalent resistance R_{eq}	Stator resistance R_1	Rotor resistance $R_2 = R_{eq} - R_1$	c
cps		ohms	ohms	ohms	
60	1.00	0.548	0.187	0.361	....
55	1.19	0.527	0.184	0.343	3.42
50	1.44	0.502	0.181	0.321	3.74
45	1.78	0.480	0.178	0.302	3.62
40	2.25	0.456	0.175	0.281	3.61
35	2.94	0.434	0.172	0.262	3.50
30	4.00	0.410	0.168	0.242	3.49
25	5.76	0.389	0.165	0.224	3.38
20	9.00	0.365	0.162	0.203	3.78
				Average value of c	3.57

R_{eq} obtained from curve, Figure 7.

$R_1 = R_{1dc}\left[1 + (f - 10)0.004\right]$, where $R_{1dc} = 0.156$ ohm.

$$c = \frac{(f_1/f_2)^2 R_{2_1}(R_{2_2} - R_{2dc}) - R_{2_2}(R_{2_1} - R_{2dc})}{R_{2dc}\left[(f_1/f_2)^2(R_{2_2} - R_{2dc}) - (R_{2_1} - R_{2dc})\right]}$$

TABLE VI

NO-LOAD TEST

Line current I	Terminal voltage V_t	Power input P_{in}
amperes	volts	watts
10.00	230	312
9.30	220	320
8.14	200	264
6.80	174	208
5.65	150	200
4.59	125	148
3.60	100	120
2.93	80	100
2.30	60	86
1.85	44	70
1.72	30	58
2.14	20	60

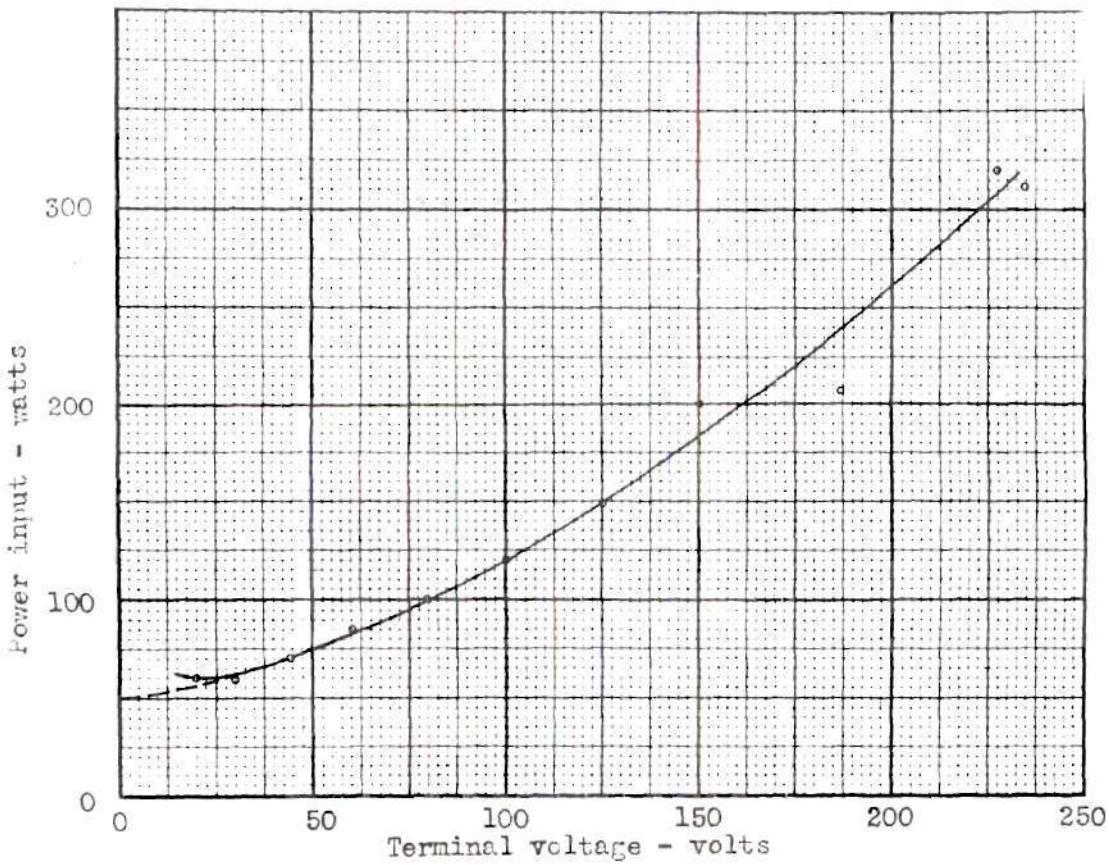

FIGURE 8

DETERMINATION OF FRICTION AND WINDAGE LOSS

losses both become zero with no excitation.

From this plot, friction and windage loss was found to be 50 watts.

Determination of magnetizing impedance. The magnetizing impedance was found in the normal manner from a full voltage no-load test. From Table VI and using the approximate equivalent circuit with the magnetizing impedance connected across the terminals,

$$Z_m' = \frac{V}{I} = \frac{228}{\sqrt{3} \times 10.3} = 12.8 \text{ ohms} \tag{19}$$

$$R_m' = \frac{P_{in}}{3I^2} = \frac{300}{3 \times 10.3^2} = 0.94 \text{ ohm} \tag{20}$$

$$X_m' = \sqrt{12.8^2 - 0.94^2} = 12.8 \text{ ohms} \tag{21}$$

More accurately, this impedance should be connected between the stator and rotor, and the stator impedance should be subtracted from the above values:

$$R_m = 0.94 - R_1 = 0.75 \text{ ohm} \tag{22}$$

$$X_m = 12.8 - X_1 = 12.3 \text{ ohms} \tag{23}$$

The above R_m includes the friction and windage loss, while it should represent core loss alone. Subtracting the 50 watt friction and windage loss from the 300 watt input,

$$R_m = \frac{250}{3 \times 10.3^2} - 0.19 = 0.79 - 0.19 = 0.60 \text{ ohm.} \tag{24}$$

Substituting these values in the equivalent circuit, the exact circuit of Figure 9 and the approximate circuit of Figure 10 are obtained.

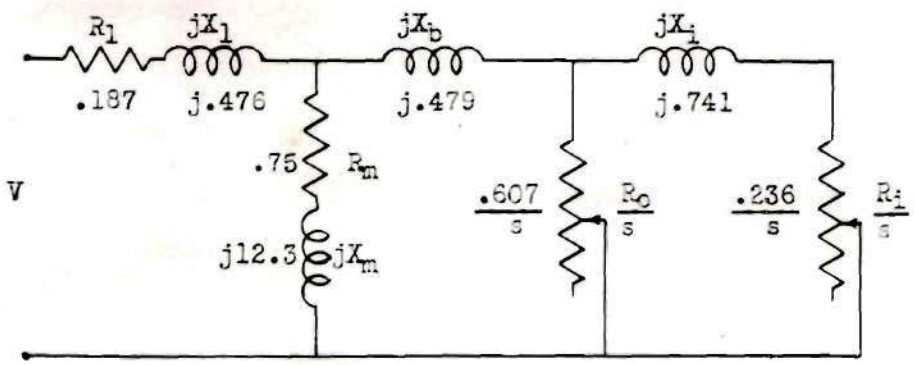

FIGURE 9

EXACT EQUIVALENT CIRCUIT

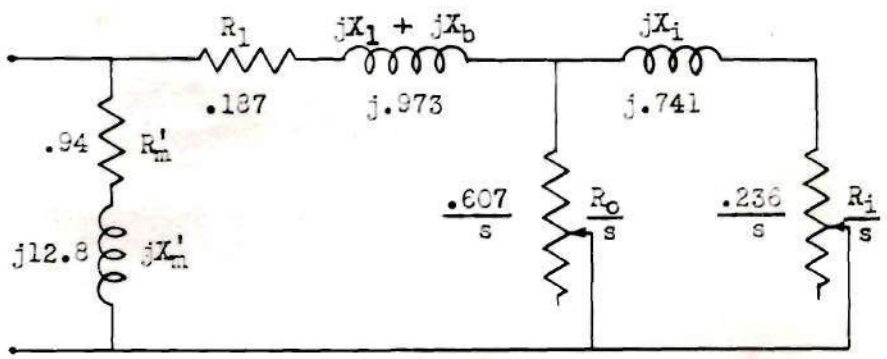

FIGURE 10

APPROXIMATE EQUIVALENT CIRCUIT

CHAPTER IV

DEVELOPMENT OF THE CURRENT DIAGRAM

In this chapter, three current diagrams will be developed: one using the approximate equivalent circuit of Figure 10; a second using the more exact diagram of Figure 9; and the last using the method prescribed by the AIEE test code.

Current diagram developed from approximate equivalent circuit.[1] The complete current locus for the approximate equivalent circuit was obtained by successive inversions.[2] Referring to the diagram, Figure 11, coordinate axes were drawn about point O', reactances being measured horizontally and resistances vertically. The inner cage reactance X_i (0.741 ohm) was laid off to the right of O' and R_i/s upward from the end of X_i. This line so drawn forms the locus of the inner cage impedance Z_i. In a like manner, the outer cage impedance Z_o could be drawn. These two loci were then inverted about O', Z_i giving the circle Y_i and Z_o giving the straight line through the origin, Y_o. Corresponding values (i.e., for equal slip) of Y_i and Y_o were then added vectorially, giving the combined admittance locus Y_{oi}. This was then re-inverted about O', and the impedance $R_1 + j(X_1 + X_b)$ added by shifting the origin down the distance R_1 (0.187 ohm), and to the left $X_1 + X_b$ (0.973 ohm), giving a new origin O". The distance from the new origin O" to any point on the curve Z_{oi} gives the total impedance $Z_1 + Z_2$. This locus was then inverted about O", giving the admittance of this part of the

---

[1] M. G. Say and E. N. Pink, The Performance and Design of Alternating Current Machines (London: Sir Isaac Pitman & Sons, Ltd., 1936), pp. 274-78.

[2] Cf. Appendix II, p. 63.

circuit. The magnetizing admittance was then included by shifting the origin to 0, by means of moving down a value g_m (0.0057 mho) and to the left b_m (0.0782 mho). The resulting distances from this origin 0 to the curve Y represent the total admittance of the equivalent circuit; when these are multiplied by the phase voltage, the line current is obtained.

For small values of slip, the locus Z_{oi} is nearly a straight line; thus its inversion is very close to being the arc of a circle. Furthermore, since Z_{oi} in this range is vertical, the center of this circle lies on the horizontal line through 0", and was found geometrically. A slip line for this portion of the current diagram was found by extending Z_{oi} downward and finding a fictitious point for infinite slip; this point was then inverted about 0", giving the point Y'_{∞}. From this point Y'_{∞} lines were drawn to the center of the circle, to the origin 0" (where s = 0), and through the point on Y where s = 0.1. The slip line was then drawn perpendicular to this radius and divided linearly with "s" as shown. With this device, the slip for any point on the circular part of the current locus may be found by drawing a line from the point in question to the point Y'_{∞}; the intersection of this line with the slip line gives the slip directly. It should be emphasized that this is true only over the circular part of the current locus.

The torque line was then drawn so the vertical distance from it to the horizontal line through 0" was proportional to the stator I^2R loss. Where the current locus is a circle, the torque line is straight; at large slips, when the current locus is no longer a circle, the torque line was obtained by plotting several points so that the distance above the horizontal meets the above condition. For example, at s = 0.5, current, from the diagram, equals 99.5 amperes. Stator I^2R loss is

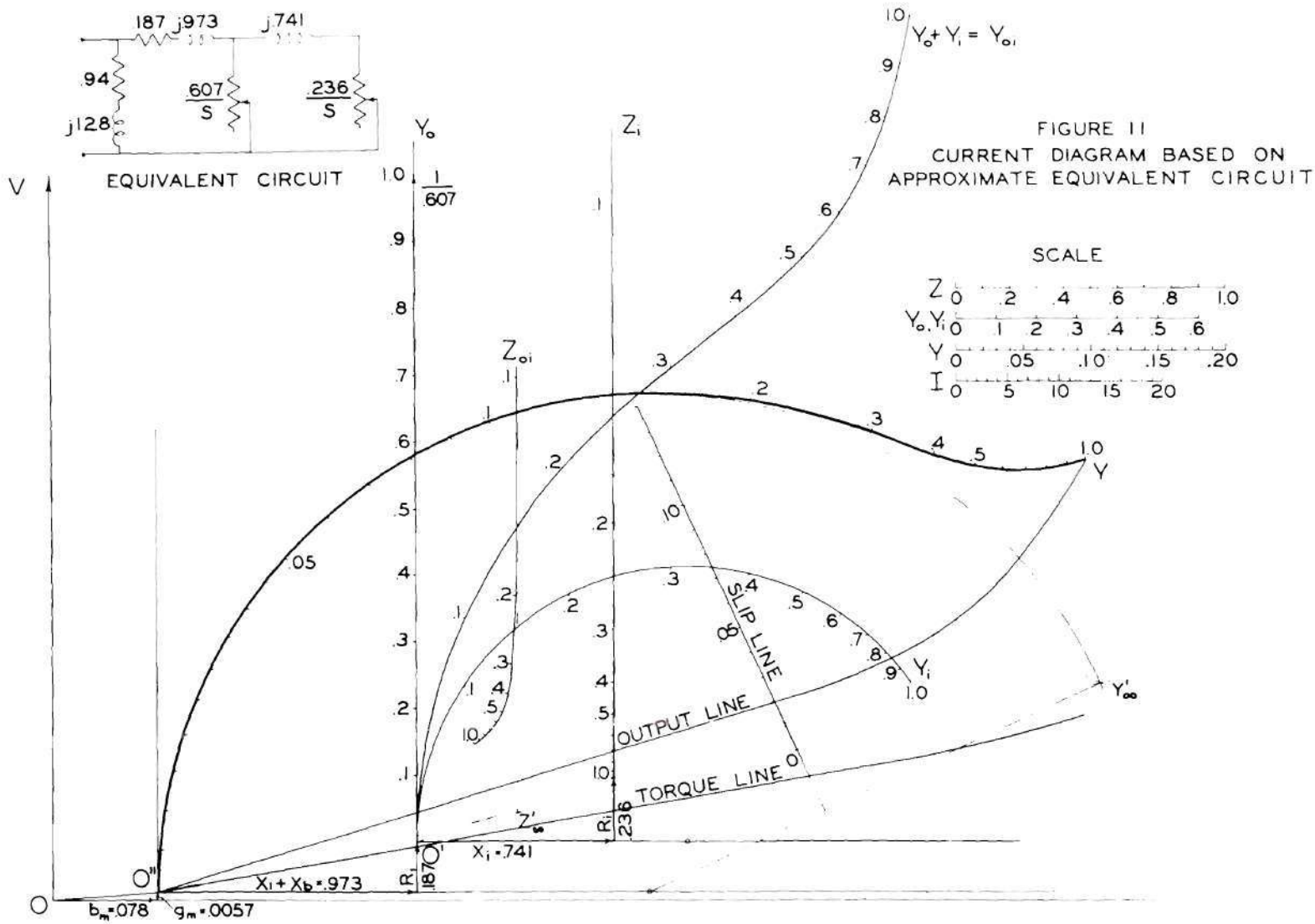

FIGURE 11
CURRENT DIAGRAM BASED ON
APPROXIMATE EQUIVALENT CIRCUIT

then 99.5^2 x 0.187, or 1850 watts; converting this to the current scale of the diagram, 1850/131 = 14.1 amperes. This distance was laid off in the proper place, several other points found and plotted, and the torque curve drawn through them.

The power output is found by multiplying output torque by 1 - s. The torque for a number of values of slip was measured, multiplied by 1 - s, and laid off downward from the current locus. At s = 0.5, torque in synchronous watts equals 131 x 27.0; therefore P = (1 - 0.5)131 x 27.0 equals 131 x 13.5; 13.5 amperes is then laid off beneath the current locus at s = 0.5.

The diagram thus produced is read just as the ordinary circle diagram for the single cage machine. In this case, the torque line and power output line give delivered torque and power, since the windage and friction loss is included with the core loss in g_m.

Current diagram developed from exact equivalent circuit. A more accurate current diagram may be obtained by using the exact equivalent circuit of Figure 9, page 25, according to the method devised by Krondl.[3] "Exact" is somewhat a misnomer; many assumptions are still present.

In this method, the rotor equivalent circuit is simplified to the form shown in Figure 12, page 31, where

$$Z_2 = R_b/s + jX_b + \frac{(R_o'/s)jX_i'}{R_o'/s + jX_i'} \tag{25}$$

$$R_b = \frac{R_o R_i}{R_o + R_i} \tag{26}$$

$$R_o' = \frac{(R_o)^2}{R_o + R_i} \tag{27}$$

---

3 Milan Krondl, "Das Arbeitsdiagramm des Boucherot-Motors," Elektrotechnik und Maschinenbau, 49:161-67, March 1, 1931.

$$jX_i' = jX_i\left(\frac{R_o}{R_o + R_i}\right)^2 \tag{28}$$

Taking the real axis vertically upward and the imaginary axis horizontally to the left, equation (25) plotted gives the sum of a vertical straight line R_b/s and a circle $\frac{(R_o'/s)jX_i'}{R_o'/s + jX_i'}$, both with the parameter "s",[4] displaced from the origin by jX_b. This impedance is shown in Figure 13.

For small values of slip, thus for the operating range, jX_i' in the denominator of equation (25) is small compared to R_o'/s, and may be neglected. Equation (25) then becomes:

$$Z_2 = \frac{R_b}{s} + j(X_b + X_i') \tag{29}$$

Thus, for small slips, the curve from equation (25) may be replaced by a straight line (K_o' in Figure 13), which is also the asymptote of the curve.

The circle of curvature for the point $s = \infty$ passes very close to the point for $s = 1$; it can with very small error be passed through these two points, giving the shape of the curve for large slips as the circle K_∞'. At $s = \infty$, from equation (25), $Z_2 = jX_b$.

Numerically, the values obtained from equations (26) through (28) were in this case

$$R_b = \frac{R_o R_i}{R_o + R_i} = \frac{0.607 \times 0.236}{0.607 + 0.236} = 0.170 \text{ ohm} \tag{30}$$

$$R_o' = \frac{R_o R_o}{R_o + R_i} = \frac{0.607^2}{0.607 + 0.236} = 0.437 \text{ ohm} \tag{31}$$

---

[4] Michael Liwschitz-Garik and Clyde C. Whipple, Electric Machinery (New York: D. Van Nostrand Company, Inc., 1946), II, 512-14.

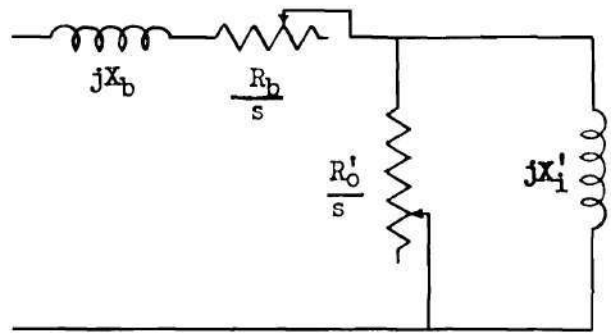

FIGURE 12

MODIFIED EQUIVALENT CIRCUIT
(ROTOR)

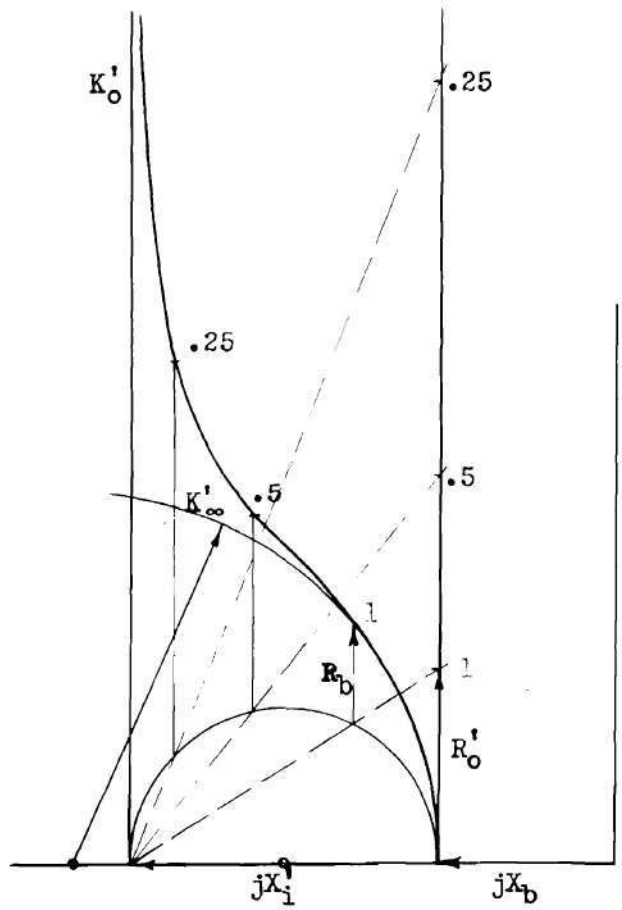

FIGURE 13

IMPEDANCE DIAGRAM FOR MODIFIED CIRCUIT

$$X_i' = X_i\left(\frac{R_o}{R_o + R_i}\right)^2 = 0.741\left(\frac{0.607}{0.607 + 0.236}\right)^2 = 0.384 \text{ ohm} \qquad (32)$$

The equivalent circuit then has the values as shown in Figure 14.

The current diagram was developed from this circuit by using the relationships[5]

$$I = I_n + \frac{V}{Z'} \qquad (33)$$

$$Z' = R_1 + jX_1(1 + \tau_1) + Z_2(1 + \tau_1)^2 \, e^{-j2\alpha} \qquad (34)$$

where I = line current,

I_n = ideal no-load current (mechanical losses = 0)

$$\alpha = \text{arc tan} \frac{R_1}{X_m + X_1} \qquad (35)$$

$\tau_1 = X_1/X_m$, primary leakage coefficient, (36)

X_m = magnetizing reactance,

R_1 = stator effective resistance,

X_1 = stator leakage reactance,

Z_2 = rotor impedance as given by Figure 13, page 31.

The current diagram was then obtained by first plotting Z' as obtained from Figure 13 and equation (34). This is the diagram shown at the left in Figure 14. The curve Z' was then inverted about the origin, multiplied by V as prescribed by equation (33), and the ideal no-load current I_n added by shifting the origin.

The slip line, torque line, and power output line were then drawn as described for the approximate diagram.[6] In this case, however, the torque line and power output line give developed torque and power,

---

[5] Krondl, op. cit., pp. 163-64.

[6] Cf. pp. 27-29.

and the actual power output determined by drawing a power-delivered line parallel to the output line and a distance above it representing phase friction and windage loss.[7]

In preparation for drawing Figure 14, the following values were determined from the equivalent circuit and equations (33) through (36):

$$\tau_1 = \frac{X_1}{X_m} = \frac{0.476}{12.3} = 0.039 \tag{37}$$

$$(1 + \tau_1)^2 = (1.039)^2 = 1.079 \tag{38}$$

$$\tan \alpha = \frac{R_1}{X_m + X_1} = \frac{0.187}{12.3 + 0.476} = 0.0146 \tag{39}$$

$$X_i'(1 + \tau_1)^2 = 0.384 \times 1.079 = 0.414 \text{ ohm} \tag{40}$$

$$X_b(1 + \tau_1)^2 = 0.497 \times 1.079 = 0.536 \text{ ohm} \tag{41}$$

$$R_o'(1 + \tau_1)^2 = 0.437 \times 1.079 = 0.471 \text{ ohm} \tag{42}$$

$$R_b(1 + \tau_1)^2 = 0.170 \times 1.079 = 0.183 \text{ ohm} \tag{43}$$

$$X_1(1 + \tau_1) = 0.476 \times 1.039 = 0.495 \text{ ohm} \tag{44}$$

In Figure 14, the circle K_o is the inversion of the straight line K_o'; it corresponds to the circle diagram of a single cage motor with rotor impedance as given by equation (29). The circle K_a is the inversion of the straight line K_a'; it corresponds to the diagram for a single cage machine with rotor reactance jX_b. The circle K_∞ is the inversion of the circle K_∞'; it is tangent to the circle K_a, and inversion of the point of tangency and one other is sufficient to define its location. The transition curve from K_o to K_∞ may be plotted point by point, or it may be sketched in by making a logical guess, as suggested by Krondl.[8]

---

[7] Liwschitz and Whipple, op. cit., p. 202.

[8] Krondl, op. cit., p. 164.

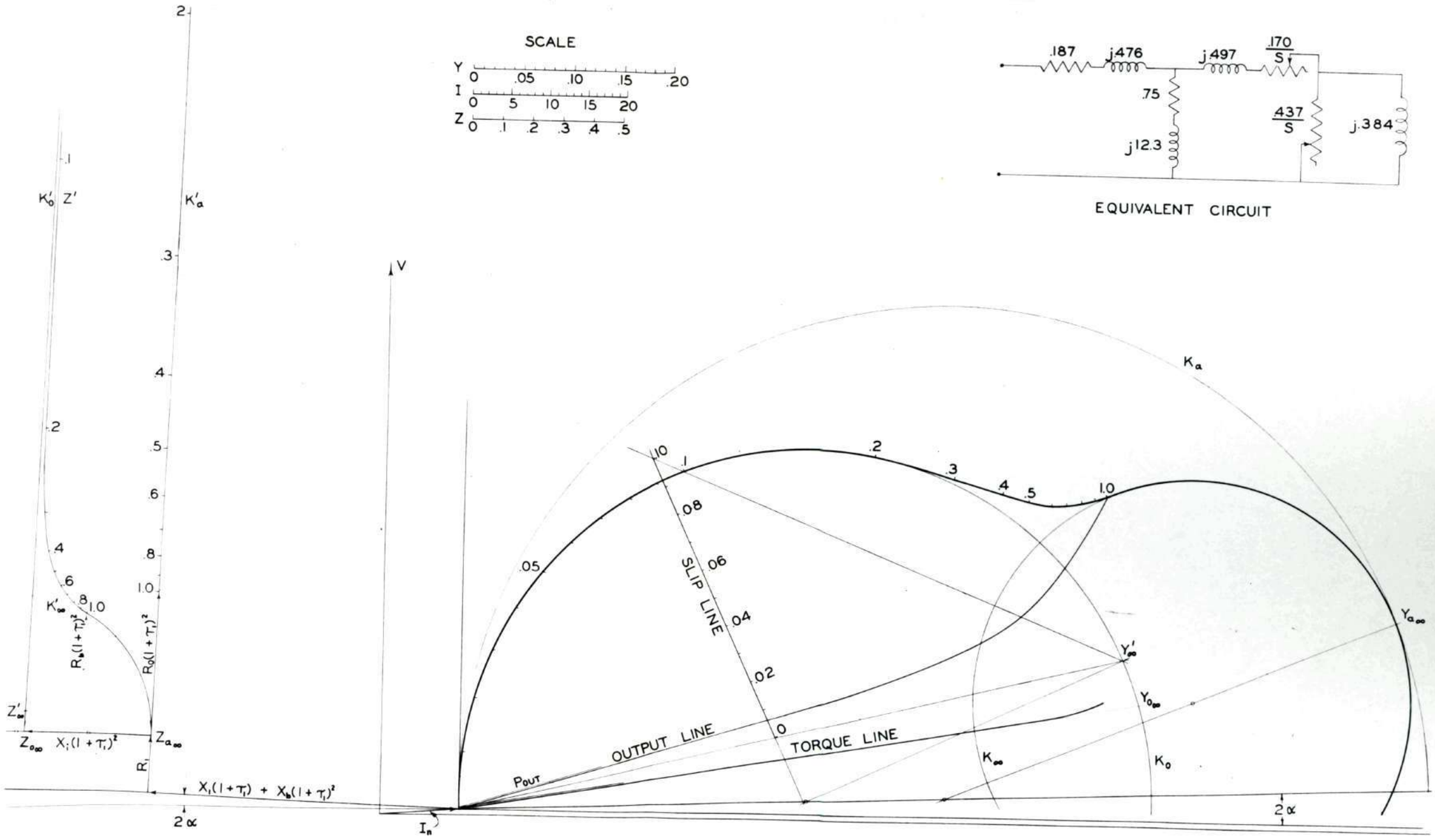

FIGURE 14
CURRENT DIAGRAM BASED ON
EXACT EQUIVALENT CIRCUIT

AIEE method. The method prescribed by the AIEE Standards[9] uses the equivalent circuit shown in Figure 15, which is the same circuit used for a single cage machine. The constants, however, are found from a reduced frequency blocked-rotor test, preferably at 15 cycles; the equivalent resistance thus obtained is used, and the equivalent reactance is found by multiplying the low-frequency reactance by the ratio of the normal frequency to the test frequency.

In this manner and using the data of the blocked test of Table IV, page 19,

$$X_{eq} = (f_1/f_2)\, X_{eq_2} = (60/15)\ 0.437 = 1.75 \text{ ohm} \qquad (45)$$

Due to the very low frequency of this test, the d-c resistance of the stator was used as the effective stator resistance. Thus,

$$R_2 = R_{eq} - R_{1dc} = 0.340 - 0.156 = 0.184 \text{ ohm} \qquad (46)$$

The ratio of 1.2 between the 60-cycle effective resistance and the d-c resistance of the stator was again assumed, giving

$$R_1 = R_{1dc} \times 1.2 = 0.156 \times 1.2 = 0.187 \text{ ohm} \qquad (47)$$

The equivalent circuit with constants designated and the circle diagram plotted therefrom (in the usual manner[10]) are shown in Figure 15.

---

[9] AIEE Test Code for Polyphase Induction Machines (AIEE Standards No. 500, New York: American Institute of Electrical Engineers, 1937), p. 9.

[10] Albert F. Puchstein and Tom C. Lloyd, Alternating Current Machines (New York: John Wiley & Sons, Inc., 1942), pp. 266-70

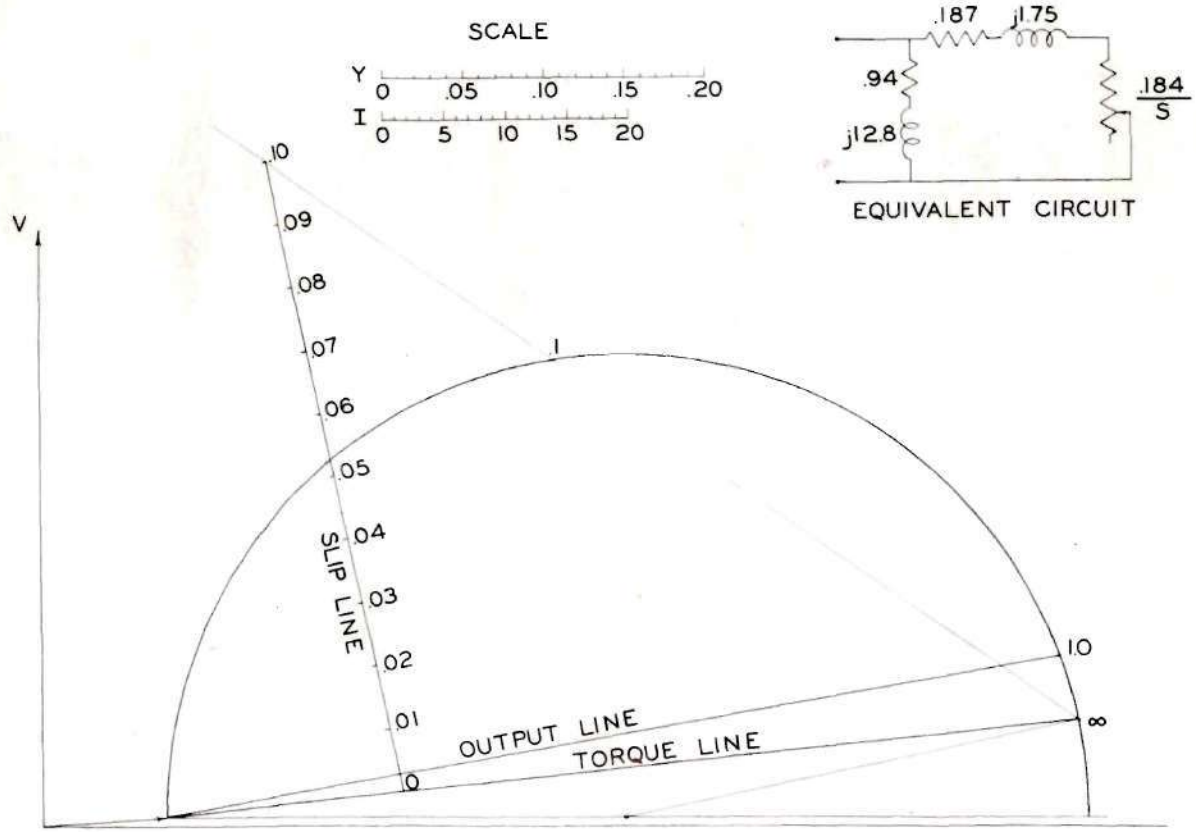

FIGURE 15
CURRENT DIAGRAM BASED
ON AIEE METHOD

CHAPTER V

COMPARISON OF PREDICTED AND ACTUAL CHARACTERISTICS

In order to compare the predicted characteristics with the actual operating performance, two methods were used. In the operating range, a brake test was performed. To obtain data at high slip, instantaneous values of current and speed were measured on starting. These two sets of data were then compared with the predicted values obtained from the three current diagrams.

Performance in operating range. The results of the brake test are given in Table VII, and the predicted data from each of the current diagrams in Tables VIII, IX, and X. Choosing slip as the independent variable, since it was felt that it was one of the more accurately measured quantities of the brake test, curves of line current, torque, power input, and power output were plotted versus slip from each of the three methods. These are shown in Figures 16 through 19, pp. 43-46. The points spotted on these curves are those obtained from the brake test.

Performance at high slips. Instantaneous values of current and speed during starting were measured with a Brush Magnetic Direct-Inking Oscillograph. The current element was actuated by the voltage drop across a resistor, and an a-c voltage proportional to speed was obtained by using a small drag-cup motor as a tachometer. This is a two-phase induction motor; with one phase excited with a constant alternating voltage, the voltage induced in the other phase is directly proportional to the speed. This has the advantage over an ordinary a-c tachometer in that frequency generated is constant and not also a function of speed.

The oscillogram so obtained is shown in Figure 20, page 47, and data obtained from it is plotted in Figure 21, which also shows the predicted curves obtained from the approximate and exact equivalent circuit current diagrams.

Though there is no test data to compare with, complete torque-slip curves are also shown in Figure 21, plotted by each of the three methods.

TABLE VII

RESULTS OF BRAKE TEST

Slip	Current	Torque	Power output	Power input	Effi-ciency	Power factor
	amperes	lb.-ft.	kw.	kw.	%	%
.0020	10.3	2.8	.71	.84	85	20.8
.0028	10.5	4.0	1.02	1.14	90	27.5
.0044	10.9	5.5	1.40	1.68	84	39.2
.0061	11.6	7.5	1.90	2.23	85	49.0
.0067	11.7	8.2	2.08	2.36	88	51.4
.0083	12.9	9.5	2.41	2.82	86	55.6
.0105	13.9	11.6	2.94	3.55	83	65.0
.0122	14.9	13.5	3.40	3.92	87	67.0
.0128	15.2	14.5	3.65	3.90	93	65.3
.0150	16.9	16.5	4.15	4.76	87	71.8
.0195	19.7	20.5	5.14	6.00	86	77.5
.0222	20.8	23.5	5.87	6.40	92	78.3
.0261	25.0	27.5	6.84	7.40	92	75.4
.0266	24.5	26.5	6.60	7.50	88	78.0
.0278	24.5	27.5	6.83	7.66	89	79.5
.0294	25.5	28.6	7.08	8.16	87	81.5
.0320	28.7	31.8	7.85	8.52	92	75.5
.0330	28.3	33.0	8.15	8.96	91	80.5
.0360	30.7	34.5	8.50	9.50	89	78.6

TABLE VIII

PREDICTED DATA USING APPROXIMATE EQUIVALENT CIRCUIT

Slip	Current	Torque	Power output	Power input	Efficiency	Power factor
	amperes	lb.-ft.	kw.	kw.	%	%
.000	10.2	0.0	0.00	0.31	0.0	7.8
.005	11.5	6.2	1.60	1.90	84.2	42.0
.010	14.0	11.9	3.04	3.40	89.5	61.8
.015	17.2	17.8	4.48	4.95	90.5	73.3
.020	20.6	23.0	5.71	6.34	90.5	78.4
.025	24.1	27.8	6.95	7.67	90.5	81.0
.030	27.4	32.1	7.93	8.85	89.7	82.2
.035	30.9	36.6	8.96	10.10	88.7	83.4
.040	34.2	40.4	9.84	11.18	88.0	83.2
.045	37.4	43.6	10.60	12.15	87.2	82.6
.050	40.4	46.6	11.28	13.08	86.2	82.4
.100	63.0	61.6	14.10	18.28	77.1	73.8
.200	84.0	57.7	11.80	19.05	61.9	57.8
.300	92.1	49.9	8.91	17.81	50.0	49.2
.400	96.5	44.6	6.85	16.95	40.4	44.7
.500	99.5	41.6	5.30	16.54	32.0	42.3
.600	101.8	40.2	4.12	16.38	25.2	40.9
.700	103.8	39.2	2.98	16.38	18.2	40.1
.800	105.8	38.6	1.96	16.48	11.9	39.7
.900	107.9	38.2	0.98	16.63	5.9	39.2
1.000	109.6	38.0	0.00	16.80	0.0	39.1

TABLE IX

PREDICTED DATA USING EXACT EQUIVALENT CIRCUIT

Slip	Current	Torque devel.	Torque deliv.	Power deliv.	Power input	Efficiency	Power factor
	amperes	lb.-ft.	lb.-ft.	kw.	kw.	%	%
.000	10.2	0.2	0.0	0.00	0.30	0.0	7.5
.005	11.1	5.7	5.5	1.40	1.75	80.0	40.1
.010	13.2	11.1	10.9	2.73	3.14	87.0	60.6
.015	16.2	16.6	16.4	4.12	4.58	90.0	72.0
.020	19.2	21.6	21.4	5.35	5.92	90.3	78.5
.025	22.4	26.2	26.0	6.50	7.15	91.0	81.3
.030	25.6	30.5	30.3	7.52	8.34	90.2	83.0
.035	28.8	34.6	34.4	8.50	9.47	89.7	83.8
.040	31.8	38.2	38.0	9.32	10.50	88.8	84.2
.045	34.7	41.4	41.2	10.04	11.48	87.5	84.3
.050	37.6	44.5	44.3	10.70	12.35	86.6	83.7
.100	59.2	60.1		13.73	17.55	78.3	75.7
.200	79.2	57.5		11.70	18.52	63.2	59.6
.300	86.5	50.9		9.05	17.50	51.8	51.6
.400	91.2	46.3		7.05	16.80	42.0	47.0
.500	93.6	43.8		5.55	16.38	33.9	44.6
.600	95.0	42.5		4.33	16.22	26.7	43.5
.700	98.0	42.0		3.20	16.28	19.7	42.4
.800	100.0	41.8		2.11	16.42	12.9	41.9
.900	101.8	41.4		1.03	16.58	6.2	41.5
1.000	103.3	41.0		0.00	16.73	0.0	41.2

TABLE X

PREDICTED DATA USING AIEE METHOD

Slip	Current	Torque	Power output	Power input	Efficiency	Power factor
	amperes	lb.-ft.	kw.	kw.	%	%
.000	10.2	0.0	0.00	0.30	0.0	7.5
.005	11.3	5.4	1.39	1.74	80.0	39.2
.010	13.4	10.7	2.68	3.07	87.3	58.4
.015	16.2	15.9	3.98	4.37	91.1	68.7
.020	19.2	20.6	5.25	5.66	92.6	75.0
.025	22.2	24.7	6.20	6.77	91.6	76.8
.030	25.4	28.9	7.20	7.87	91.5	78.9
.035	28.4	32.3	8.06	8.85	91.1	79.4
.040	31.3	35.6	8.85	9.76	90.6	79.4
.045	34.3	38.6	9.55	10.57	90.5	78.5
.050	36.8	41.1	10.13	11.35	89.3	78.5
.100	56.5	51.8				
.200	72.2	43.4				
.300	77.7	33.3				
.400	80.0	26.6				
.500	81.5	21.9				
1.000	84.1	8.1				

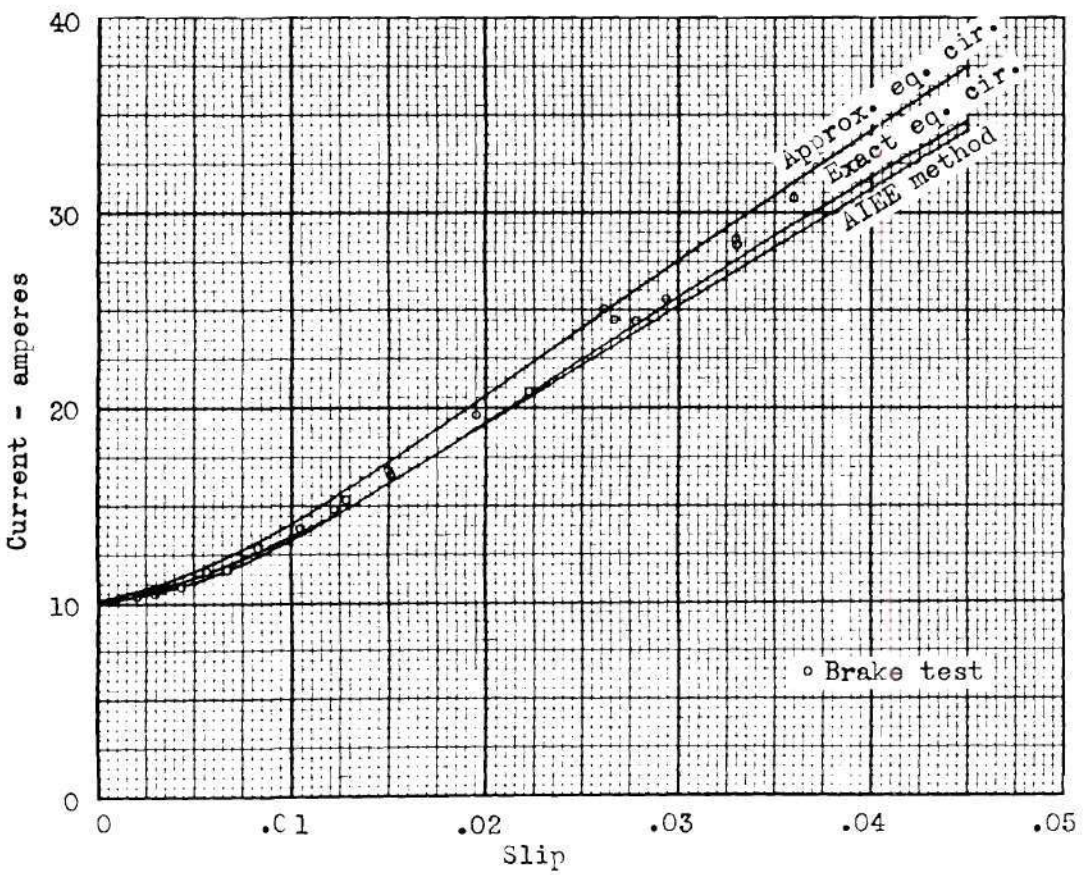

FIGURE 16

CURRENT VS. SLIP -- PREDICTED AND FROM TEST

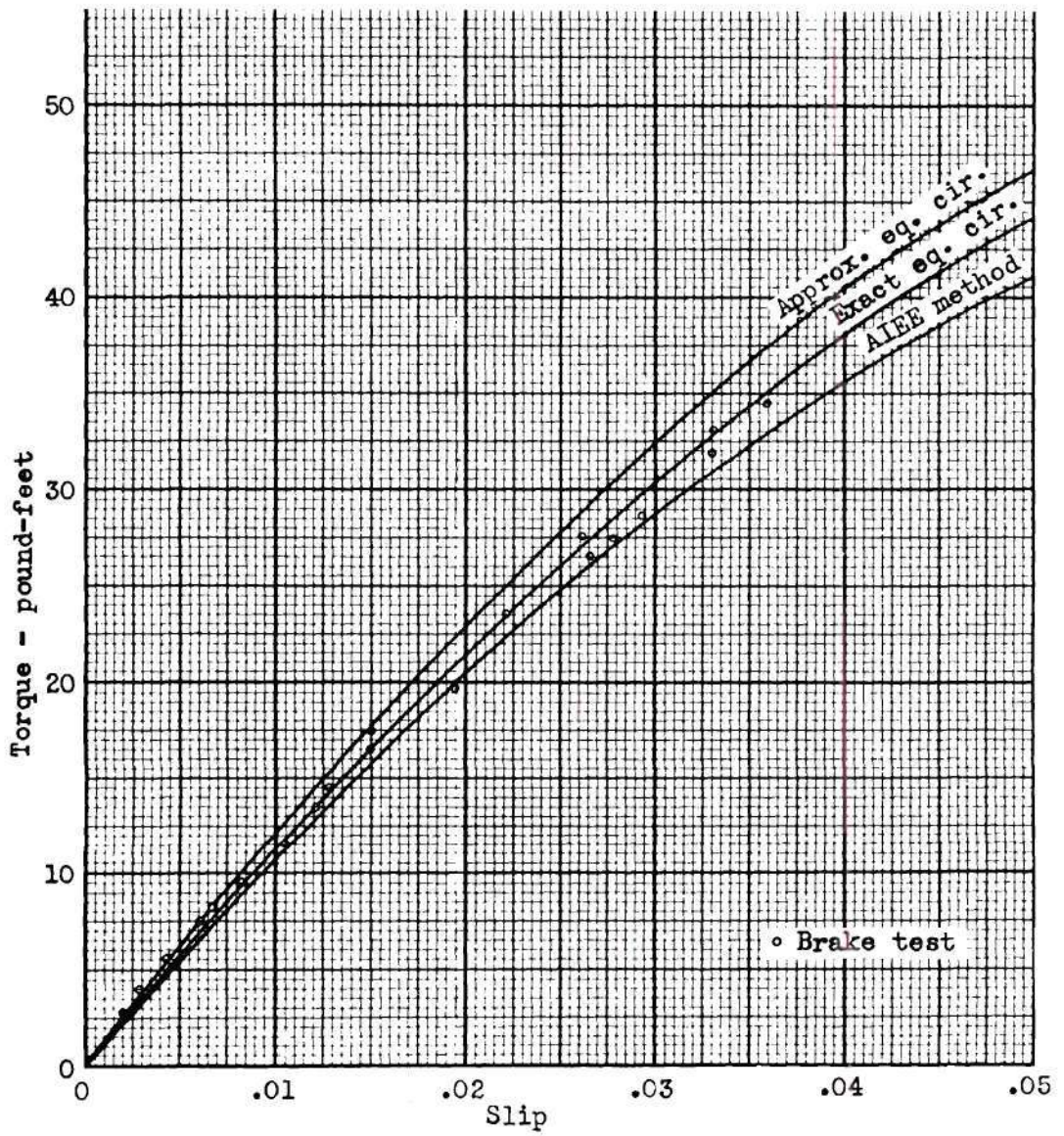

FIGURE 17

TORQUE VS. SLIP --PREDICTED AND FROM TEST

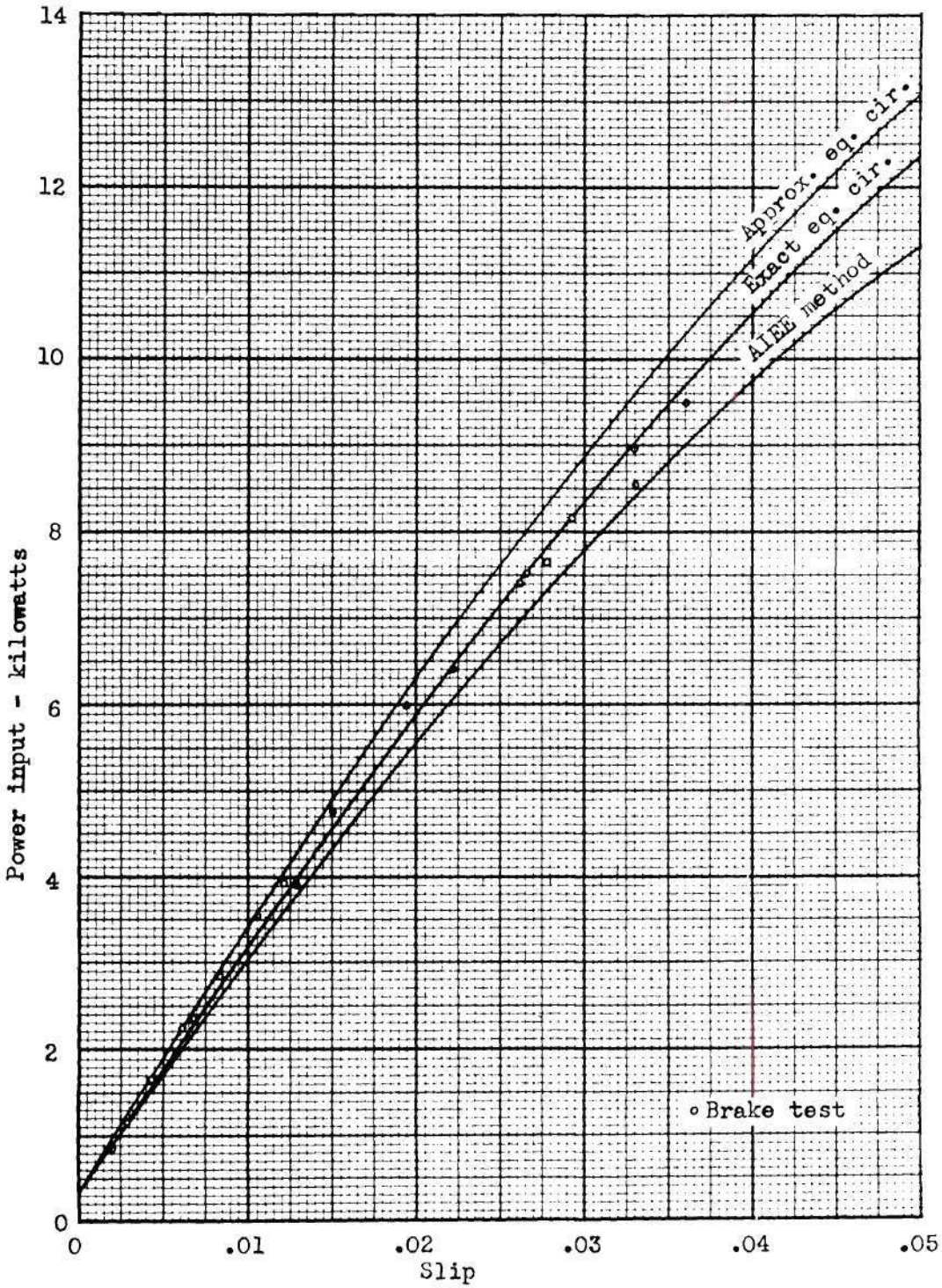

FIGURE 18

POWER INPUT VS. SLIP -- PREDICTED AND FROM TEST

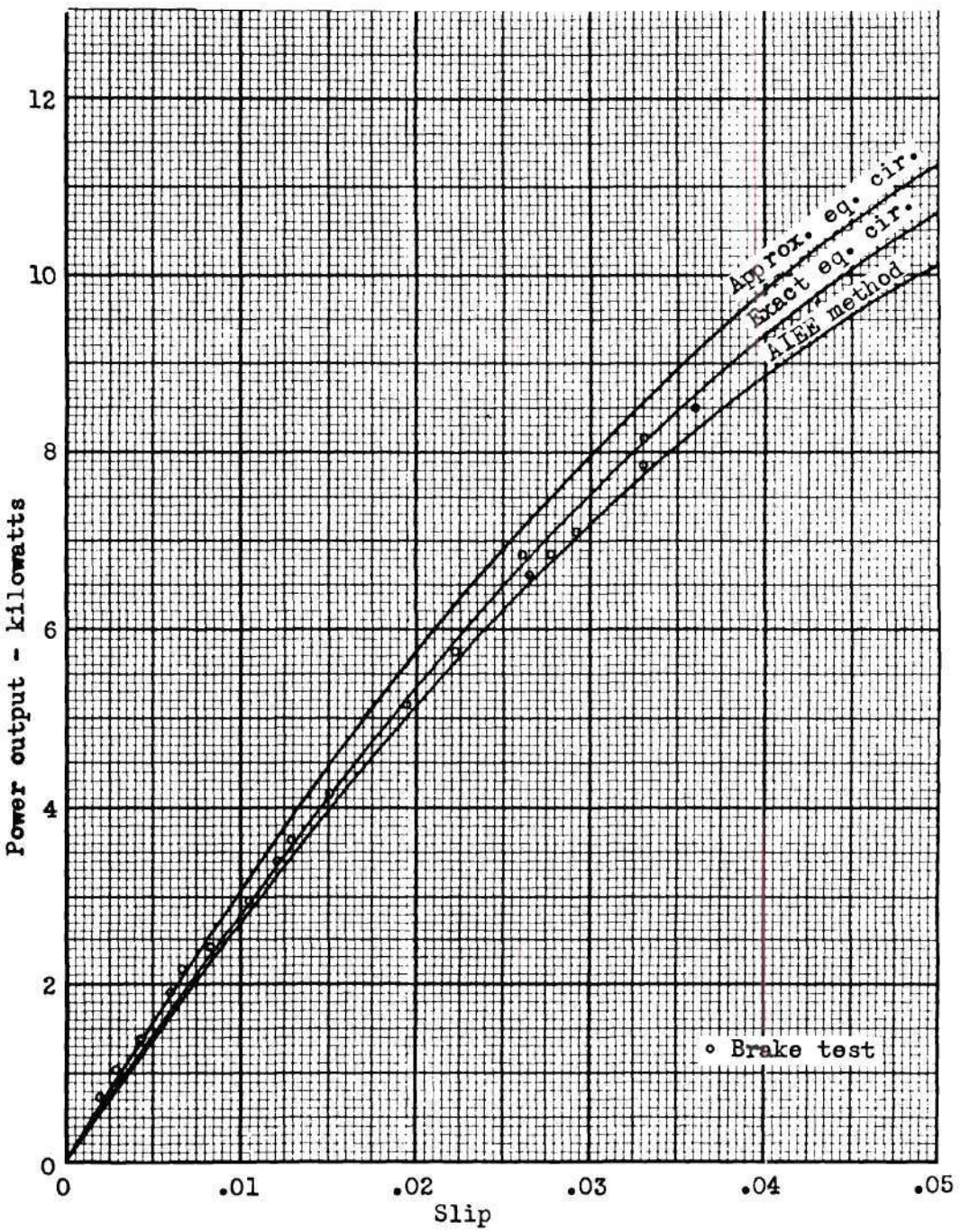

FIGURE 19

POWER OUTPUT VS. SLIP -- PREDICTED AND FROM TEST

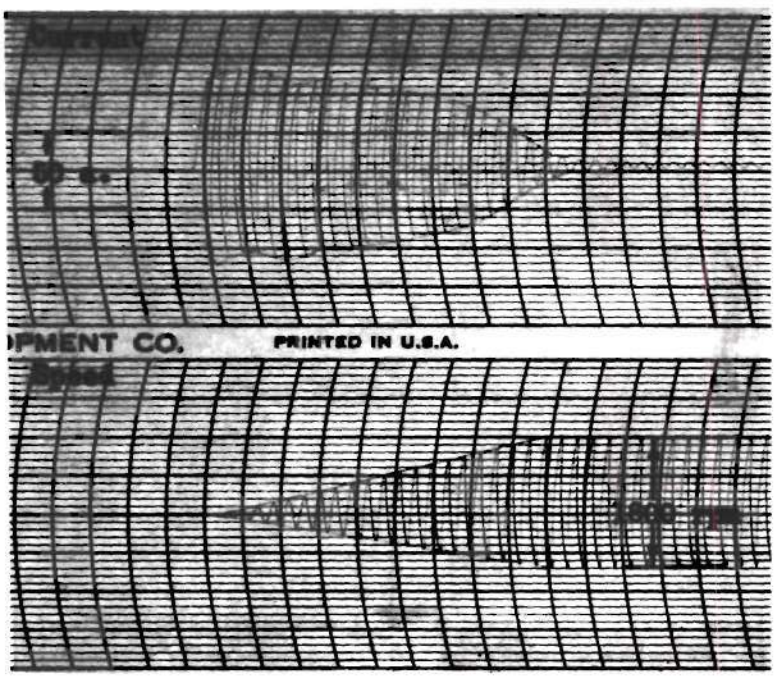

FIGURE 20

OSCILLOGRAMS OF CURRENT AND SPEED ON STARTING

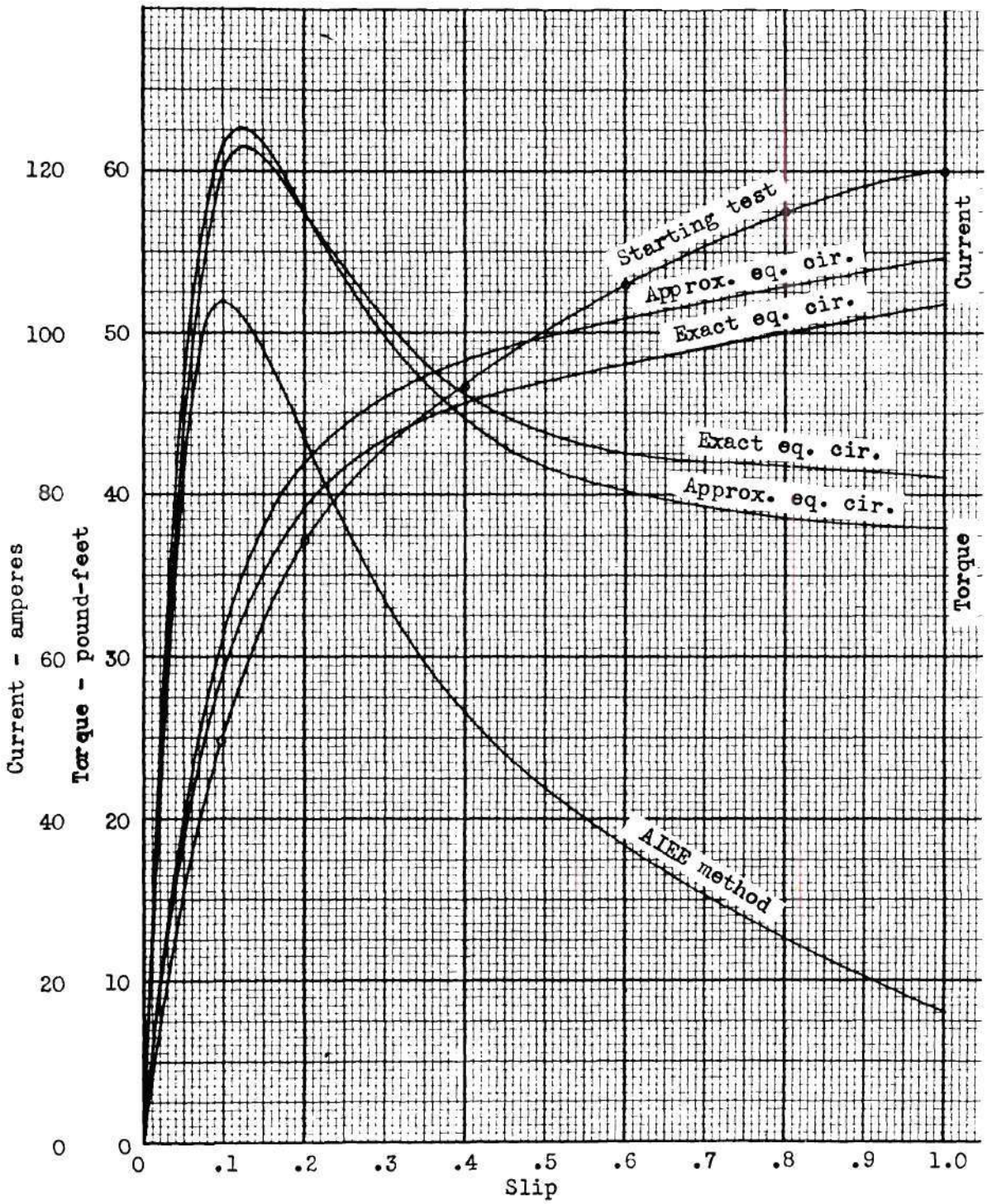

FIGURE 21

TORQUE AND CURRENT VS. SLIP -- LARGE SLIPS

CHAPTER VI

ANALYSIS OF RESULTS OBTAINED

Comparison of accuracy of methods. Referring to the curves of Figures 16 to 19, the method developed by Krondl using the exact equivalent circuit gave the best results, as would be expected. Certainly its accuracy is as good as that of the brake test, which gave some rather scattered points.

The approximate circuit gave results not far from those of the exact circuit. It would be sufficient for most uses, but it is questionable that using it is any less work than using the more accurate exact diagram, since the main task is in initially determining the constants. There is little difference in the labor involved in plotting the diagrams. It will be noted that the results were very good in spite of the rather large variation of the constant "c".

The AIEE method gave surprisingly good results in the operating range. It is felt that this is partially coincidence, since with the many assumptions involved it is hard to believe that this method would consistently give such good results. At higher slips the method falls down completely, since the ordinary circle it is based upon can make no allowances for the changing rotor resistance involved.

The values obtained for current vs. slip at large values of slip did not check as well as those in the operating range. The starting test itself is of limited accuracy, however. Also, the probable saturation of the iron at these high values of current would permit a greater current flow than that predicted from the current diagrams, since these were developed assuming negligible saturation.

Varying temperature was a rather unpredictable source of error.

It was attempted to make all tests at or convert to the same temperature, but nonetheless this is thought to be one of the largest single sources of error.

Meters used were standard laboratory grade instruments, on the average of one-half percent accuracy. It was neccessary to use current transformers with the meters available, and these introduced another source of error.

Possibilities for further research. It would be desirable to perform the identical tests outlined above on other double-cage machines, as a check on the several somewhat empirical relationships used, particularly in the AIEE method.

The method outlined above for separation of rotor and stator resistances suggests the possibility of applying this same principle to ordinary induction motors to determine the ratio of effective to d-c resistance of each, rather than assuming the ratios equal as is often done.

It would be interesting to extend the test performed during starting to include torque and power measurements. Power could be measured with a filament type oscillograph with a power element; instantaneous torque would be more difficult to measure. Two possibilities would be by means of a brake arm pressing on a carbon pile resistor or moving a spring-loaded potentiometer slider. These both involve the possible errors due to the inertia of the brake arm and the static friction of the brake on the pulley.

BIBLIOGRAPHY

BIBLIOGRAPHY

AIEE Test Code for Polyphase Induction Machines, (AIEE Standards No. 500). New York: American Institute of Electrical Engineers, 1937. 26 pp.

Alexanderson, E. F. W., "General Characteristics of Ship Propulsion Apparatus," General Electric Review, 22:224-32, April, 1919.

Arnold, E., Die Wechselstromtechnik, V., 2. Berlin: Julius Springer, 1912. 659 pp.

Baffrey, R., "Der Doppelkäfigankermotor," Elektrotechnik und Maschinenbau, 46:749-54, July 8, 1928

Behrend, B. A., The Induction Motor. New York: McGraw-Hill Book Company, Inc., 1921. 272 pp.

Krondl, Milan, "Das Arbeitsdiagramm des Boucherot-Motors," Elektrotechnik und Maschinenbau, 49:161-67, March 1, 1931.

Langsdorf, Alexander S., Theory of Alternating-Current Machinery. New York: McGraw-Hill Book Company, Inc., 1937. 788 pp.

Lawrence, Ralph R., Principles of Alternating-Current Machinery. New York: McGraw-Hill Book Company, Inc., 1940. 678 pp.

Liwschitz-Garik, Michael, and Clyde C. Whipple, Electrical Machinery, Vol. II, New York: D. Van Nostrand Company, Inc., 1946. 576 pp.

Örley, D., and G. Jekelfalussy, "Practical Design of Double Squirrel Cage Motors," Engineers' Digest, 4:253-56, June, 1947. Translation from Elektrotechnika, 38:108-13, December 15, 1946.

Puchstein, Albert F., and Tom C. Lloyd, Alternating-Current Machines. New York: John Wiley & Sons, Inc., 1942. 655 pp.

Punga, Franklin, "Die günstigste Dimensionierung des Boucherot-Motors," Archiv für Elektrotechnik, 21:1, January 1928.

Punga, Franklin, and Otto Raydt, Modern Polyphase Induction Motors. London: Sir Isaac Pitman & Sons, Ltd., 1933. 289 pp.

Say, M. G., and E. N. Pink, The Performance and Design of Alternating Current Machines. London: Sir Isaac Pitman & Sons, Ltd., 1936. 552 pp.

Standard Handbook for Electrical Engineers. New York: McGraw-Hill Book Company, Inc., 1941. 2303 pp.

Steinmetz, Charles P., Theory and Calculation of Electrical Apparatus. New York: McGraw-Hill Book Company, Inc., 1917. 480 pp.

Voigt, Hanskarl, "Die Trennung der Widerstände eines Doppelkäfig-Ankers," Elektrotechnik und Maschinenbau, 50:133-35, February 28, 1932.

_____, "Vereinfachung des Leerlaufverfahrens zur Bestimmung des Läuferwiderstandes von Asynchronmotoren," Elektrotechnik und Maschinenbau, 49:167-68, March 1, 1931.

Wall, T. F., "Squirrel Cage Induction Motors with High Starting Torque and Low Starting Current," Engineering (London), 116:164-66, August 10, 1923.

APPENDICES

APPENDIX I

DERIVATION OF EQUATIONS USED

Equation for determination of rotor resistance.[1] The power input to an induction motor with a small load is found by

$$P_i = P_{fe_1} + P_{cu_1} + P_{cu_2} + P_f + P_p + P_o \qquad (A1)$$

where P_{fe_1} = stator iron loss

P_{cu_1} = stator copper loss

P_{cu_2} = rotor copper loss

P_f = friction & windage

P_p = tooth pulsation loss

P_o = power output

Of this, the portion P_{fe_1} and P_{cu_1} will be consumed in the stator and the remainder, transferred across the air gap, is

$$P_2 = P_{cu_2} + P_f + P_p + P_o \qquad (A2)$$

Of this, a portion P_h is lost in the iron and $P_2' = P_2 - P_h$ is delivered to the rotor copper.

Figure 22 is a plot of $P_i' = P_i - P_{cu_1}$ as a function of slip. At small slips this is a straight line; at synchronous speed, there is a discontinuity equal to $2P_h$. P_2', the power delivered to the rotor copper, is as shown.

P_2' is also given by the expression

---

[1] Hanskarl Voigt, "Vereinfachung des Leerlaufverfahrens zur Bestimmung des Läuferwiderstandes von Asynchronmotoren," Elektrotechnik und Maschinenbau, 49:167-68, March 1, 1931.

$$P_2' = \frac{R_{2dc}}{s}(I_2)^2 \tag{A3}$$

Inserting the expression for rotor current,

$$I_2 = \frac{E}{\sqrt{(R_{2dc}/s)^2 + X_2{}^2}} \tag{A4}$$

equation (A3) becomes,

$$P_2' = \frac{E^2 R_{2dc}}{s\left[(R_{2dc}/s)^2 + X_2{}^2\right]} \tag{A5}$$

Since at small slip $X_2{}^2$ is negligible with respect to $(R_{2dc}/s)^2$,

$$R_{2dc} = \frac{E^2 s}{P_2'} \tag{A6}$$

In this equation, s/P_2' is the reciprocal of the slope of the line in Figure 22; any two points on the line will determine this slope. Thus to evaluate the rotor resistance, it is neccessary only to measure the power input and slip at no load and at a very small load. Several points should of course be taken to minimize experimental error.

Writing equation (A6) in terms of slope,

$$R_{2dc} = E^2 \frac{\Delta s}{\Delta P_2'} \tag{A7}$$

Derivation of constants used in separation of resistances of the two cages.[2] Referring to the equivalent circuit and notation of Figure 2, the rotor impedance may be expressed as:

$$Z_2 = \frac{R_o/s(R_i/s + jX_i)}{R_o/s + R_i/s + jX_i} + jX_b \tag{A8}$$

---

[2] Hanskarl Voigt, "Die Trennung der Widerstände eines Doppelkäfig-Ankers," Elektrotechnik und Maschinenbau, 50:133-35, February 28, 1932.

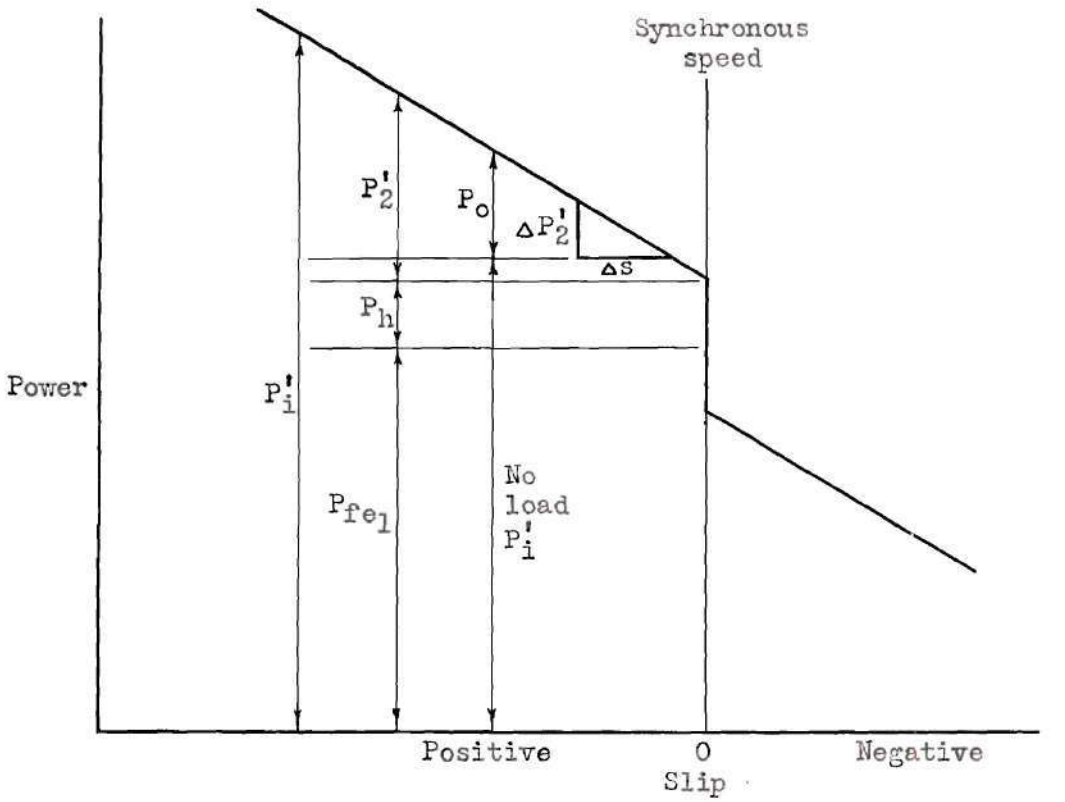

FIGURE 22

POWER INPUT COMPONENTS PLOTTED VERSUS SLIP

Introducing the constants,

$$c = 1 + \frac{R_o}{R_i} \tag{A9}$$

$$v = \frac{X_i}{R_i} \tag{A10}$$

equation (A8) becomes:

$$Z_2 = \frac{R_o}{s}\left(\frac{R_i + jX_i s}{R_o + R_i + jX_i s}\right) + jX_b \tag{A11}$$

$$= \frac{R_o}{s}\left(\frac{1 + jvs}{c + jvs}\right) + jX_b \tag{A12}$$

Separating into real and imaginary parts,

$$Z_2 = \frac{R_o}{s}\,\frac{(1 + jvs)(c - jvs)}{c^2 + (vs)^2} + jX_b \tag{A13}$$

$$= \frac{R_o}{s}\,\frac{c + (vs)^2}{c^2 + (vs)^2} + j\left[X_b + R_o v\,\frac{c - 1}{c^2 + (vs)^2}\right] \tag{A14}$$

With the rotor blocked, s = 1 and equation (A14) becomes:

$$Z_2 = R_o\,\frac{c + v^2}{c^2 + v^2} + j\left[X_b + R_o v\,\frac{c - 1}{c^2 + v^2}\right] \tag{A15}$$

$$= R_2 + jX_2 \tag{A16}$$

where R_2 and X_2 represent effective rotor resistance and reactance. R_o and c are independent of frequency; X_b and v are directly proportional to frequency when unsaturated conditions are assumed.[3]

By a blocked rotor test at frequency f_1 the effective rotor resistance is determined to be R_{2_1}; at frequency f_2 to be R_{2_2}. Then,

$$R_{2_1} = R_o\,\frac{c + v^2}{c^2 + v^2} \tag{A17}$$

---

[3] Michael Liwschitz-Garik and Clyde C. Whipple, Electric Machinery (New York: D. Van Nostrand Company, Inc., 1946), Vol. II, p. 214.

$$R_{2z} = R_o \frac{c + (f_2/f_1)^2 v^2}{c^2 + (f_2/f_1)^2 v^2} \tag{A18}$$

For frequency f = 0, i.e. direct current, $f_2/f_1 = 0$, and the direct current resistance of the rotor is

$$R_{2dc} = R_o/c \tag{A19}$$

R_{2dc} is determined from the light load test as described in the first section of this appendix; so equations (A17), (A18), and (A19) are three equations in the three unknowns R_o, c, and v. Simultaneous solution of these three equations gives

$$c = \frac{(f_1/f_2)^2 R_{21}(R_{2z} - R_{2dc}) - R_{2z}(R_{21} - R_{2dc})}{R_{2dc}\left[(f_1/f_2)^2(R_{2z} - R_{2dc}) - (R_{21} - R_{2dc})\right]} \tag{A20}$$

From this equation c is calculated and substituted in equation (A19) to give the resistance of the outer cage as

$$R_o = cR_{2dc} \tag{A21}$$

From equation (A9), the resistance of the inner cage is

$$R_i = cR_{2dc}/(c - 1) \tag{A22}$$

Also from the simultaneous solution above,

$$v = c\sqrt{\frac{R_{21} - R_{2dc}}{cR_{2dc} - R_{21}}} \tag{A23}$$

The reactance of the inner cage is then determined from equations (A10) and (A23).

The sum of the common rotor reactance X_b and the stator reactance may be determined from the blocked rotor test using equation (A15).

The entire leakage reactance X_{eq} equals:

$$X_{eq} = X_1 + X_2 = X_1 + X_b + R_o v \frac{c - 1}{c^2 + v^2} \qquad (A24)$$

From this expression, $X_1 + X_b$ may be found. This is the required value for use in the approximate equivalent circuit of Figure 10, while for the more exact circuit of Figure 9 the approximate relationship given by the AIEE that, for a Class B machine, $X_1 = 0.4\ X_{eq}$ is used.[4]

Simplification of exact equivalent circuit.[5] The equivalent circuit as used in the method developed by Krondl may be simplified to the form shown in Figure 12, page 31, which is identical in properties when the values are properly selected.[6]

The secondary impedance of the circuit of Figure 9 is given by:

$$Z_2 = jX_b + \frac{R_o/s\ (R_i/s + jX_i)}{R_o/s + R_i/s + jX_i} \qquad (A25)$$

This is a cubic equation; had the self-reactance of the outer cage not been neglected,[7] the corresponding expression would be a fourth power equation and considerably more difficult to handle. As is, it may be made easier to work with by performing a partial division so that:

$$Z_2 = jX_b + \frac{1}{s} \frac{R_o R_i}{R_o + R_i} + \frac{jX_i \frac{1}{s} \frac{R_o^2}{R_o + R_i}}{\frac{R_o + R_i}{s} + jX_i} \qquad (A26)$$

---

[4] AIEE Test Code for Polyphase Induction Machines (AIEE Standards No. 500. New York: American Institute of Electrical Engineers, 1937), p.21.

[5] Milan Krondl, "Das Arbeitsdiagramm des Boucherot-Motors," Elektrotechnik und Maschinenbau, 49:161-67, March 1, 1931.

[6] Cf. p. 30.

[7] Cf. p. 5.

Multiplying both numerator and denominator by $\left(\frac{R_o}{R_o + R_i}\right)^2$,

$$Z_2 = jX_b + \frac{1}{s}\frac{R_o R_i}{R_o + R_i} + \frac{\frac{R_o}{s}\frac{R_o}{R_o + R_i}\, jX_i\left(\frac{R_o}{R_o + R_i}\right)^2}{\frac{R_o}{s}\frac{R_o}{R_o + R_i} + jX_i\left(\frac{R_o}{R_o + R_i}\right)^2} \tag{A27}$$

This expression is in the form:

$$Z_2 = jX_b + R_b/s + \frac{(R_o'/s)\, jX_i'}{R_o'/s + jX_i'} \tag{A28}$$

where

$$R_b = \frac{R_o R_i}{R_o + R_i} \tag{A29}$$

$$R_o' = \frac{R_o^2}{R_o + R_i} \tag{A30}$$

$$jX_i' = jX_i\left(\frac{R_o}{R_o + R_i}\right)^2 \tag{A31}$$

The values of R_b, R_o', and jX_i' may be calculated from equations (A29) through (A31), or may be determined from a simple construction as shown in Figure 23. Referring to this Figure, the above equations are rearranged and similar triangle relationships are given without further explanation:

$$\frac{R_b}{R_i} = \frac{ED}{BC} = \frac{AD}{AC} = \frac{AO}{AH} = \frac{R_o}{R_o + R_i} \tag{A32}$$

$$\frac{R_o'}{R_o} = \frac{AG}{AO} = \frac{AE}{AB} = \frac{AD}{AC} = \frac{R_o}{R_o + R_i} \tag{A33}$$

$$\frac{FG}{OD} = \frac{AG}{AO} = \frac{AE}{AB} = \frac{AD}{AC} = \frac{AO}{AH}; \qquad \frac{OB}{OD} = \frac{CH}{OD} = \frac{AH}{AO} \tag{A34}$$

$$\frac{jX_i'}{jX_i} = \frac{FG}{OB} = \left(\frac{AO}{AH}\right)^2 = \left(\frac{R_o}{R_i + R_o}\right)^2 \tag{A35}$$

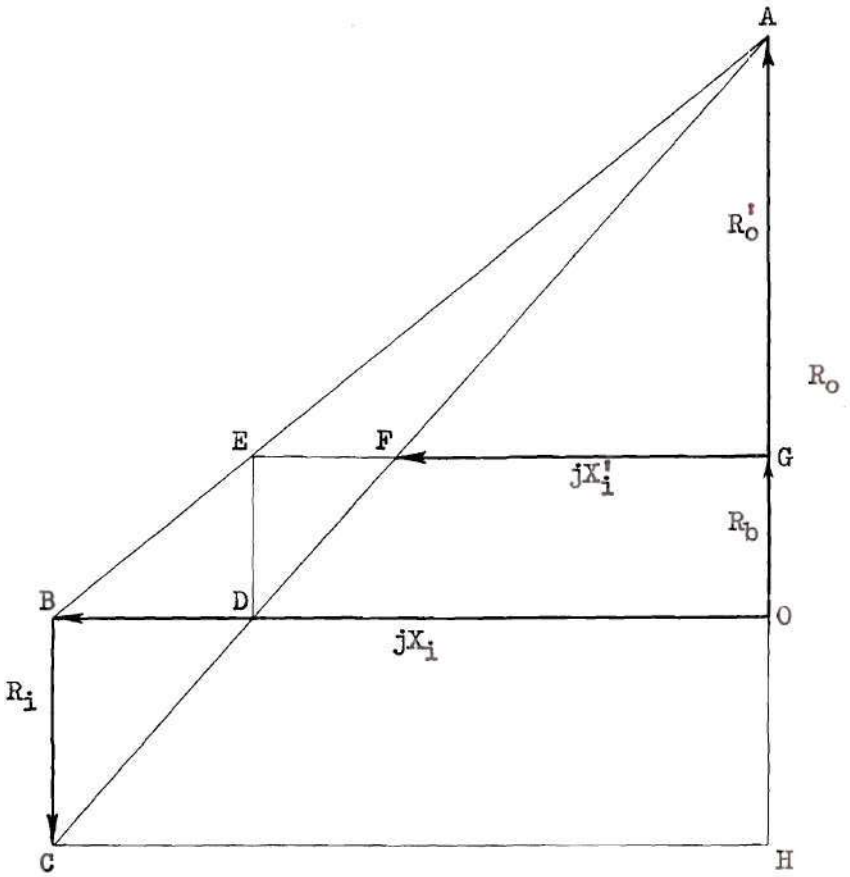

FIGURE 23

GRAPHICAL DETERMINATION OF R_b, R_o', AND jX_i'

APPENDIX II

INVERSION OF A VECTOR

The graphical method of changing from impedance to admittance is made use of several times in this thesis, and is accomplished in a simple manner.[1]

In the simplest case of a fixed value of impedance

$$\dot{Z} = Ze^{j\theta} \tag{A36}$$

$$\dot{Y} = \frac{1}{\dot{Z}} = \frac{1}{Z} e^{-j\theta} \tag{A37}$$

That is, when impedance is represented by a vector with magnitude Z at an angle θ above the reference axis, admittance is represented by a vector of magnitude $1/Z$ at an angle θ below the reference. This is known as inversion of the vector.

With a variable vector of the form,

$$\dot{Y} = \dot{V}_1 + k\dot{V}_2 \tag{A38}$$

where $\dot{V}_1$ and $\dot{V}_2$ are constant vector quantities and k is a parameter, the locus of the end points of $\dot{Y}$ are shown in Figure 24 as the line AB. Letting k take on all real values from minus to plus infinity, the inversion is:

$$\dot{W} = \frac{1}{\dot{Y}} = \frac{1}{\dot{V}_1 + k\dot{V}_2} \tag{A39}$$

This expression can be shown to be the equation of a circle, which passes

---

[1] Alexander S. Langsdorf, Theory of Alternating Current Machinery (New York: McGraw-Hill Book Company, Inc., 1937), pp. 597-602. Michael Liwschitz-Garik and Clyde C. Whipple, Electrical Machinery (New York: D. Van Nostrand Company, Inc., 1946), Vol. II, pp. 512-15.

through the origin when k equals infinity. The maximum value of $\dot{V}$ occurs when $\dot{V}$ is a minimum; that is, when $\dot{V}$ is the perpendicular to the line AB, $\dot{V}_o$. The center of the circle therefore lies on the inversion of $\dot{V}_o$, and the diameter is $1/V_o$.

Instead of using the inverted circle K, in some cases it is more convenient to use its mirror image, K'.

In like manner, the inversion of a circle through the origin is found to be a straight line, and of a displaced circle, another circle.

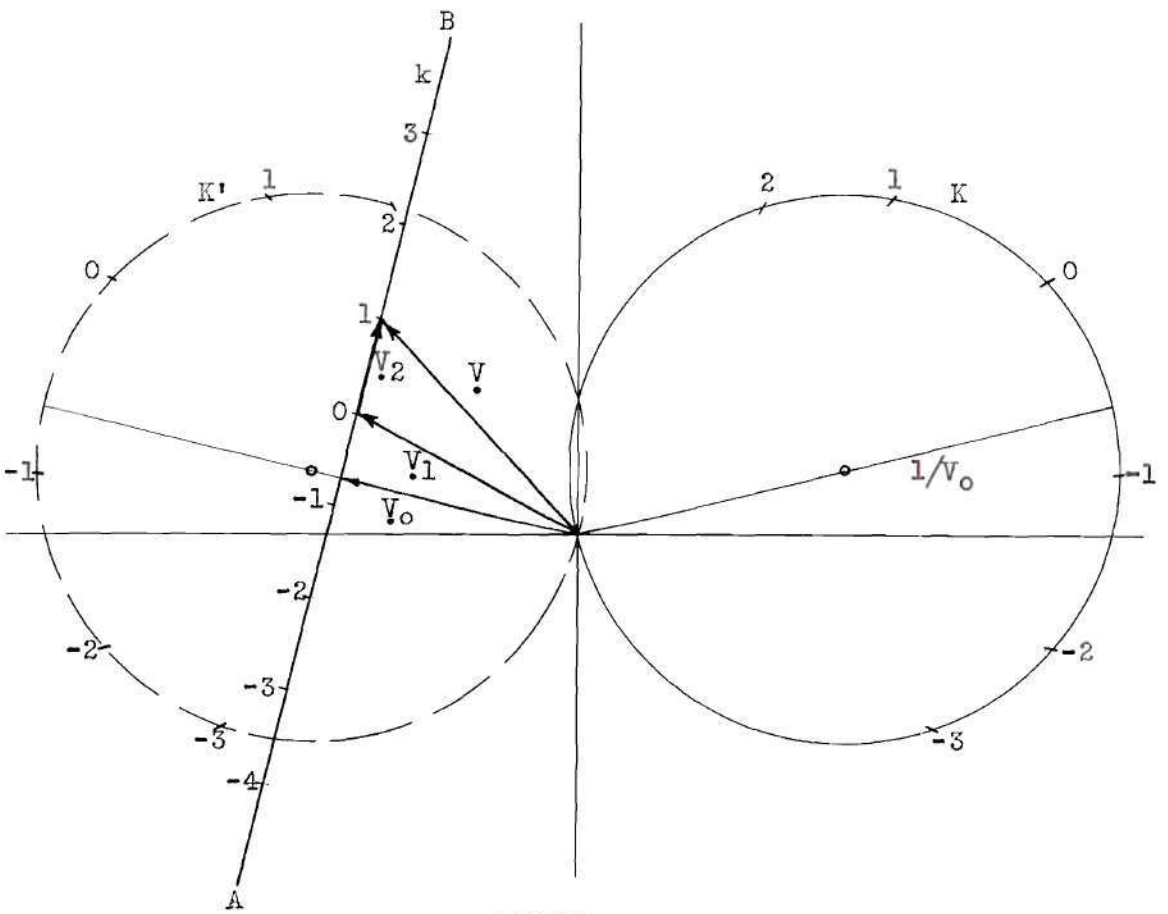

FIGURE 24

INVERSION OF A VECTOR